remote sensing

MDPI

Review

The Role of Remote Sensing in Olive Growing Farm Management: A Research Outlook from 2000 to the Present in the Framework of Precision Agriculture Applications

Gaetano Messina and Giuseppe Modica *

Dipartimento di Agraria, Università degli Studi Mediterranea di Reggio Calabria, Località Feo di Vito, I-89122 Reggio Calabria, Italy
* Correspondence: giuseppe.modica@unirc.it

Abstract: Given the importance of olive growing, especially in Mediterranean countries, it is crucial that there is a constant process of modernization aimed at both environmental sustainability and the maintenance of high standards of production. The use of remote sensing (RS) allows intervention in a specific and differentiated way in olive groves, depending on their variability, in managing different agronomic aspects. The potentialities of the application of RS in olive growing are topics of great agronomic interest to olive growers. Using the tools provided by RS and the modernization of the olive sector can bring great future prospects by reducing costs, optimizing agronomic management, and improving production quantity and quality. This article is part of a review that aims to cover the past, from the 2000s onwards, and the most recent applications of aerial RS in olive growing in order to be able to include research and all topics related to the use of RS on olive trees. As far as the use of RS platforms such as satellites, aircraft, and unmanned aerial vehicles (UAVs) as olive growing is concerned, a literature review showed the presence of several works devoted to this topic. This article covers purely agronomic matters of interest to olive farms (and related research that includes the application of RS), such as yielding and managing diseases and pests, and detection and counting of olive trees. In addition to these topics, there are other relevant aspects concerning the characterization of the canopy structure of olive trees which is particularly interesting for mechanized pruning management and phenotyping.

Keywords: olive tree detection and counting; pruning; yield; olive disease detection and pest management; unmanned aerial vehicles (UAVs) and satellite imagery; machine and deep learning

Citation: Messina, G.; Modica, G. The Role of Remote Sensing in Olive Growing Farm Management: A Research Outlook from 2000 to the Present in the Framework of Precision Agriculture Applications. *Remote Sens.* **2022**, *14*, 5951. https://doi.org/10.3390/rs14235951

Academic Editor: Peng Fu

Received: 2 September 2022
Accepted: 11 November 2022
Published: 24 November 2022

1. Introduction

Given the importance of olive growing, especially in Mediterranean countries, it is crucial that there is a constant process of modernization aimed at both environmental sustainability and the maintenance of high standards of production [1,2]. Considering the environmental risks caused by climate change with the Mediterranean region as the biggest threat, adopting available tools, best practices, and applying forward-looking policies can adapt agricultural management strategies and processes given the above mentioned changes [3]. The use of remote sensing (RS) allows intervention in a specific and differentiated way in an olive grove, depending on its variability, in managing different agronomic aspects. Remote sensed tree detection is a key factor in on-farm mapping aimed at supporting farmers in planning practices such as pruning, fertilizing, irrigation, phytosanitary treatments, and the estimation of olive productivity [4,5]. Plant breeding programs have benefited from the possibility of exploiting images from above to collect phenotypic data on plant growth and morphology, geometrical canopy characteristics, and tree vigor. These observable traits are essential in assessing the suitability of selected genotypes for cultivation in olive growing planting systems, such as modern super high-density hedges, requiring adaptability to mechanized pruning and harvesting [6,7].

One of the crucial issues concerns is the detection of plant diseases by monitoring the symptoms of olive diseases, among which two are particularly harmful as they cause severe problems to olive growing worldwide: Verticillium Wilt and Quick Decline Syndrome. The latter, caused by the now well-known plant pathogenic bacterium *Xylella fastidiosa* which has proven to cause the death of olive trees, has severe effects on the production, landscape, and cultural heritage of the territory concerned [8]. The contribution of RS in this area is to provide support in monitoring symptoms and identifying diseased trees based on a visual assessment that requires field inspections with a more significant expenditure of resources and time [9].

This review focuses on the role of aerial RS applications in olive growing farm management from the 2000s onwards.

The first review dealing with the research of RS applications in olive growing for the preservation of the olive landscape, monitoring of land use, management of irrigation resources, and environmental issues arising from olive oil mill wastes was reported in Messina and Modica [10]. This article, instead, covers purely agronomic matters of interest to olive farms, such as yielding and managing diseases and pests, detection, and counting of olive trees. In addition to these topics, there are other relevant aspects concerning the characterization of the canopy structure of olive trees, particularly interesting for mechanized pruning management and phenotyping. Therefore, the structure of the second part of this review is the following: Section 2 covers research related to methodologies for detecting and counting trees; in Section 3, pruning-related research is treated; Section 4 deals with olive yield forecast; Section 5 concerns phenotyping and monitoring of olive trees' biophysical parameters; the Section 6 focuses on monitoring and management of olive's pests and diseases; finally, Section 7 contains discussions and conclusions on the perspectives and challenges about the future of RS in olive growing. The used sources for reviewed works were the following databases: Scopus (Elsevier) Google Scholar, and Web of Science (Clarivate Analytics). Figure 1 shows the researches found, 72 in all, many of them were published in the last decade, from 2011 onward, while only a tiny fraction, just 12, were published earlier [11–22]. Of these, 11, concern tree detection and counting (discussed in Section 2) which is the topic with the highest occurrences, 27.

VOSviewer 1.6.18 software was used to perform cluster analysis on titles and abstracts (this choice is due to the lack of keywords in some of the works considered) having a frequency of at least six (Figure 2). A temporal analysis of the period under consideration (beginning of 2000–end of March 2022) was performed. However, the software detected significant occurrences only from 2014–2015, also considering the small number of articles in the first decade of the 2000s. According to the content of word occurrence, three clusters were obtained, and in line with what is covered in this review, the most common were "UAV imagery", "image", and "olive tree" followed by "olive orchards" and "accuracy assessment".

The connection is well evident between "UAV imagery" and "accuracy assessment" to which the terms "classification" and "object-based image analysis" are associated with the topic of tree detection. This connection is well-established in the pre-2017 period.

Of note is the presence of the name "Spain", indicative of the distribution of scientific work on RS in olive growing over the two decades under consideration. Figure 3 highlights the preponderant research occurrences in Spain (31), followed by Italy (17), but also a gradual broadening of research (and the increasing importance of the olive growing) in countries where olive crops are not traditional, such as Chile, Argentina, Peru, China and Australia.

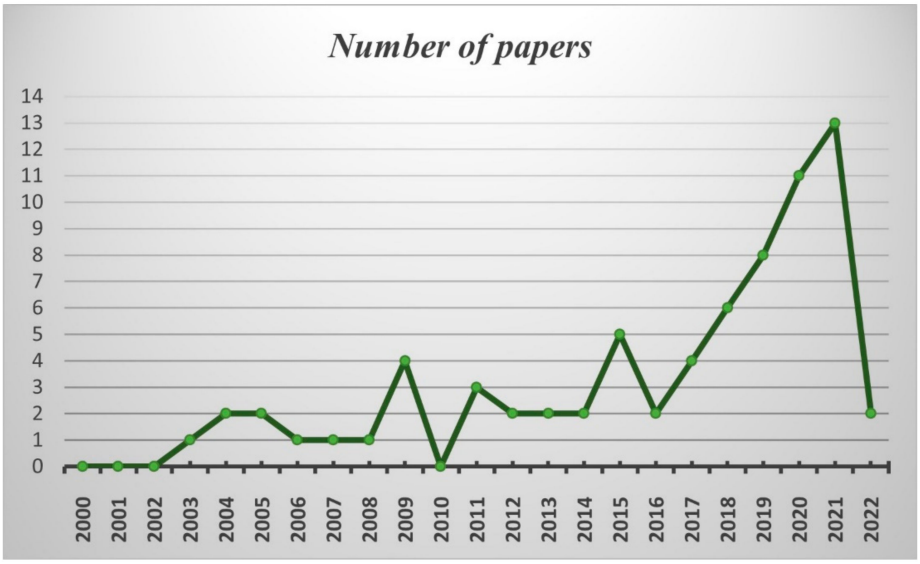

Figure 1. The trend of published articles based on publication year. The sources for the search of works reviewed were the following databases: Scopus (Elsevier) Google Scholar, and Web of Science (Clarivate Analytics). The *x*-axis shows the years of the period under consideration while the *y*-axis shows the number of researches carried out. In this review the researches considered are those carried out from the beginning of the year 2000 until the end of March 2022. Of the 72 researches in the time span analyzed, only 12 concern the years before 2011 and almost all (11) are based on tree detection and counting. The largest number of researches were carried out in the years 2020 (11) and 2021 (13).

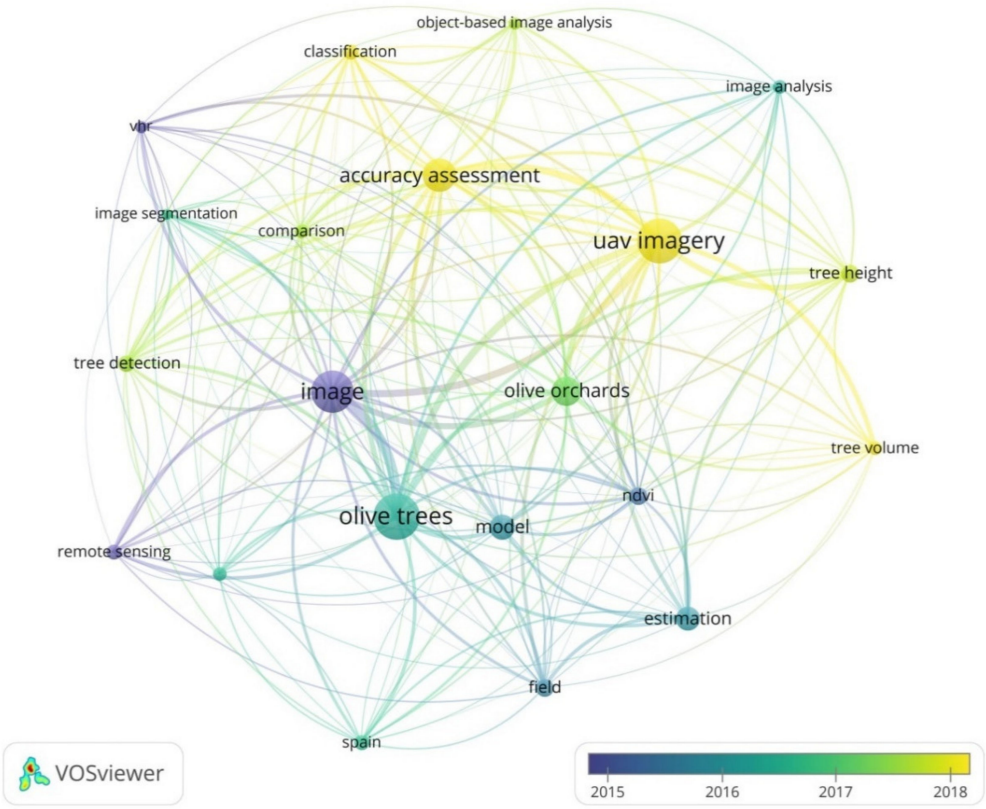

Figure 2. Keywords occurrence and clustering by VOSviewer 1.6.18. Colors indicate the year in which each title and words contained in the abstracts were more used. Lines represent co-occurrence link strength among terms.

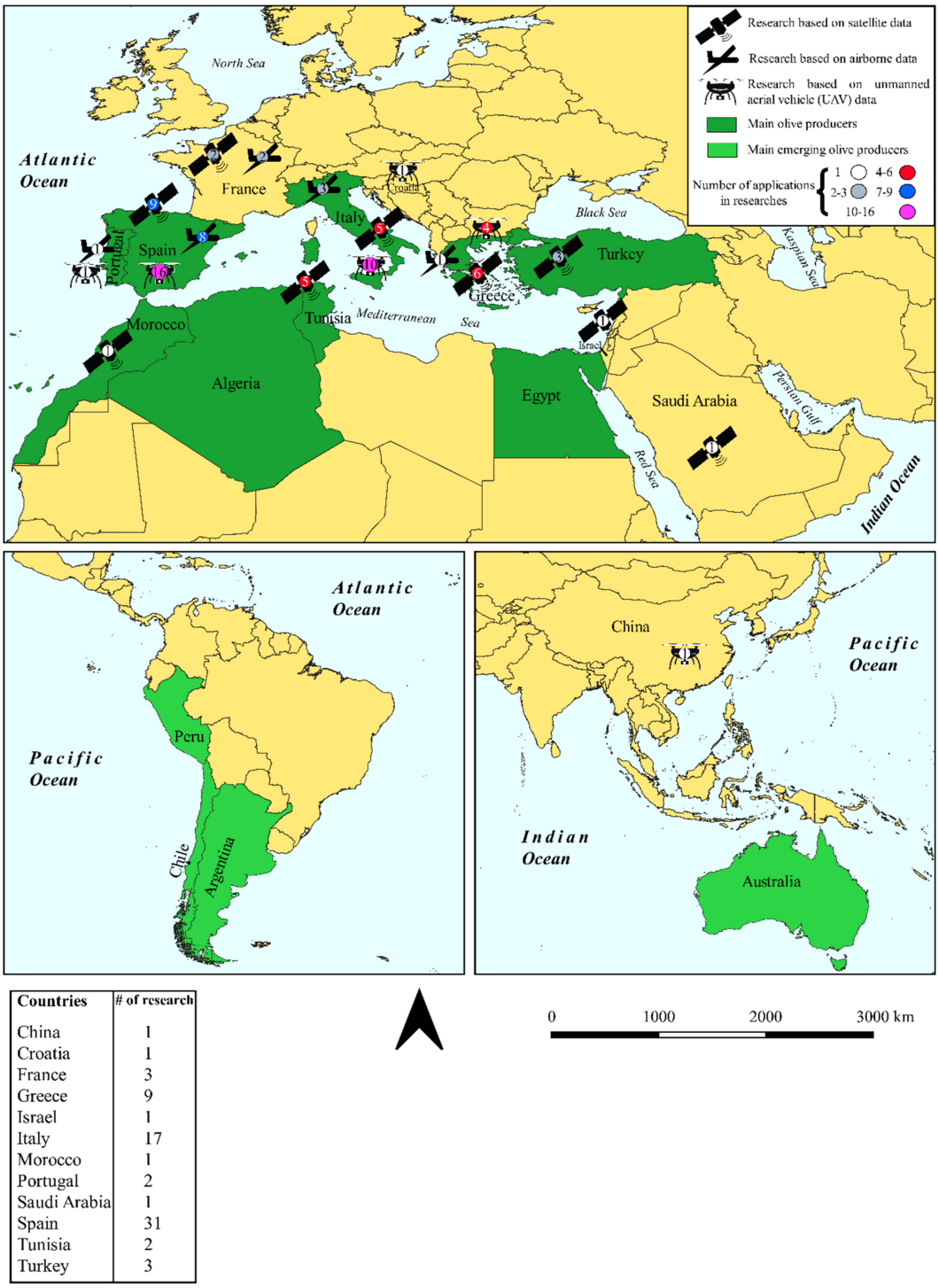

Countries	# of research
China	1
Croatia	1
France	3
Greece	9
Israel	1
Italy	17
Morocco	1
Portugal	2
Saudi Arabia	1
Spain	31
Tunisia	2
Turkey	3

Figure 3. The map shows the worldwide geographical distribution of olive cultivation and the distribution of research study sites according to the countries reported in the published papers. The main olive producer countries are highlighted in dark green, while the main emerging producer countries are highlighted in light green. The symbols of different color (shown in the upper right) distinguish the type of remote sensing (RS) platform used (satellite, airborne, or unmanned aerial vehicle) in the research and the number of researches performed from 2000 to the end of March 2022. The table at the bottom left shows the number of remote sensing researches in olive growing carried out in each country. Important to consider that some researches include the use of more than one RS platform.

The different words identified by Vosviewer, although found in some of the topics covered in this review, do not allow to encapsulate all of them. Keywords related to the topic of tree detection and phenotyping and monitoring of biophysical parameters are present. Just think of the words "tree detection", "tree height" and "tree volume" alone. However, connections to other topics that could not be overlooked given the goal of this review are missing: pruning, yield, disease detection, and pest management. Specific sections will be devoted to these topics as well.

2. Tree Detection and Counting

Tree crown detection is an important field in RS research, providing a means for species classification, vegetation distribution mapping, vegetation density estimation, and vegetation change monitoring [23]. In addition, given the economic importance of olives, especially in the Mediterranean area and considering European Union olive production subsidies, the distribution of plantations and data for estimating production require monitoring. The dynamic monitoring of the canopy in olive growing can provide information on growth and health status by exploiting vegetation indices (VIs), and is a decision support tool for the timing and mode of execution of various crop operations such as irrigation, fertilization, pruning, pest control, and yield forecasting [24]. Traditional counting methods are based on human visual inspections in the field, which are time-consuming and prone to errors, mainly when performed in large-scale plantations [25]. Since the end of the 1990s, with the launch of commercial satellites able to provide high-resolution images (< 2 m), the level of detail has become advantageous for observing smaller geographical objects such as trees. Therefore, until the end of the first decade of the 2000s, tree detection using RS techniques was performed using imagery taken by manned aircraft or satellites [16,18]. Spatial resolution is of crucial importance in the image recognition of single trees. Generally, olive trees in the productive phase have a crown diameter between 3 and 12 m, with spacing between trees variable between 8–10 m for traditional olive groves to 5 m for intensive ones, depending on the planting pattern, and trees regularly aligned [12,26,27]. Relevant data for tree counting was initially derived from panchromatic imagery with a spatial resolution between 0.6 m and 3.6 m, provided by satellites Quickbird and IKONOS and from high resolution 1:40,000 scale aircraft' flights [15,20,21]. With the advent of UAVs, these platforms are increasingly used for this application and can provide images with centimeter resolution. Most applications have regarded object detection and feature extraction for tree counting and planting line detection, recognition of planting gaps, and segmentation of invasive species. In addition, tree counting allows to geolocate plants, provide production estimates, and determine the presence of gaps [28].

According to the literature, several techniques for detecting trees were proposed, among which blob detection, template matching, image segmentation, unsupervised and supervised classification by using machine learning algorithms, and deep learning [25,29–32]. Algorithms that exploit the spatial patterns in olive groves, based on mathematical morphology operators, were tested by Barata and Pina [11] in very high spatial resolution (VHR) (1 m/pixel) RGB aerial images. Usually, researchers considered olive groves characterized by a regular spatial pattern of rows with adjacent trees placed at standard distances. In this pattern, each tree can be identified within a circular shape area if seen from above. The proposed methodologies involved the global segmentation of the olive groves to create a mask of single trees, considering olive trees as objects that do not follow the typical spatial patterns. The olive trees were segmented using a modified version of the top-hat transform [33] which identifies darker local regions against a lighter background, and allows for segmenting only the isotropic dark structures (trees) and avoiding the segmentation of directional structures like roads, water lines, or connected alignments of trees. While demonstrating a high rate in the ability to identify olive trees (89% of olive groves were correctly identified), this methodology showed limitations due to the similarity of other regular patterns that can be confused with olive trees patterns, such as fruit orchards. With a goal opposite to that of identifying individual trees Robbez-Masson and Foltête [17] aimed

to localize, using VHR aerial images missing plants in olive groves planted according to a geometrical squared-grid pattern. The parcels were considered as a topological graph of vertices, formed by centroids identified on individual plants, whose mutual position conforms to a set of geometrical rules on orientation and length. In particular, the algorithm built and used the topological and geometrical relationships between the vertices, in order to identify the "missing vertices", i.e., the missing plants.

Other authors based their tree detection on the canopies' shape. Khan et al. [29] proposed an automatic algorithm to count olive trees using satellite imagery (Quickbird) based on canopies' circular shape. Specifically, this method involved the segmentation of the image using Otsu thresholding [34] for obtaining a binary map. Olive trees were detected by exploiting their circular shape using the Circular Hough Transform (CHT) algorithm [35]. Results showed a very high overall accuracy (96%). However, the circular shape of objects other than olive trees, such as bushes, rocks, and uneven land patches, induces misclassification errors. Also, Karantzalos and Argialas [15] proposed a method for automatic olive tree extraction and counting (in IKONOS and Quickbird imagery) based on the circular shape of olive trees seen as blobs that appear brighter at the tips in the center with shadows following towards their bases. Olive tree extraction was performed after locating the local spatial maxima of the Laplacian, a differential operator exploited for edge detection along with blob detection. Trees appear as blobs in a binary image that can be labeled and counted. However, blob detection can be prone to errors since it classifies all trees with circular shapes as olive trees. In presenting their approach, Bazi et al. [22] also considered olive trees as blobs in IKONOS' imagery. Firstly, the olive trees were distinguished from other classes using a Gaussian process classifier [36], producing a binary map in which olive trees represent the primary information. Then, the map was pre-processed using the erosion morphological operator to isolate single tree canopies that were automatically counted, considering each blob valid only if its size was within a specific predetermined range referring to the actual size of trees. Similarly, Waleed et al. [30] proposed multi-step image processing techniques applied over a single (red) band for counting olive trees in Quickbird imagery. The single band was sharpened using the high pass filter and edges were detected, converting each olive tree's closed boundaries into blobs using morphological reconstruction. A binarization permitted distinguishing background from trees.

Masson et al. [12] proposed an approach based on morphological image analysis for olive tree identification in VHR imagery using airborne orthophotos, Quickbird, and IKONOS single band imagery. The morphological image analysis focuses on the pixel groups' shape and spatial arrangement. In particular, considering that tree crowns appear as dark objects, they contain a regional minimum which can be defined as a connected component of pixels whose neighbors have a higher intensity value [37]. The regional minima method was compared with the semi-automatic approach of OLICOUNT software. The software exploits an algorithm based on image spectral threshold, region growing, and tree morphological parameters. The two approaches showed similar omission errors, while the omission errors were higher for the regional minima method. The OLICOUNT software was used by Nihal et al. [13] for the detection and the semi-automatic counting of the olive trees in grey-scale input on Quickbird imagery, utilizing an algorithm based on a set of input parameters on which the shape and radiometry (grey level) depend: the minimum and maximum grey values in the image which discriminates trees from the background; the diameter range of the tree; the aspect ratio of the tree crown; the density interval that measures the size of the holes in the tree canopy concerning the total area of the tree. The results showed that OLICOUNT produced a high error for mixed (olive tree associated with other tree species), small, and irregular parcels, but less for regular parcels occupied by young olive trees.

Template matching involves the extraction of the objects of interest, such as trees, from the image if they show a match with predefined models [29]. Gonzalez et al. [19] provided an example of template matching by implementing a method of counting based on the

integration of different image analysis and probabilistic techniques tested on Quickbird imagery. In particular, the probability was calculated for olive trees present within a reticular layout and with precise geometric features such as shape, size, and the angle formed between trees. The method was based primarily on the premise that, generally, olive trees are planted following a reticular structure within the same plantation. First, it was considered a representative portion of the image in which the dark points (trees), satisfying a particular reticular layout, are located by means of a voting scheme. This step provides an estimate of how well dark point fits into the reticle. The higher is this value, the higher is the probability of a dark point to be an olive tree of the parcel represented by the selected reticle. Based on exploiting the similarity of olive trees, considering that all of them within a parcel are of the same age and probably of similar size, a prototype of the typical olive tree was obtained by processing the candidate olive trees within a representative area. The final probability that each candidate was an olive tree depended on the likelihood that the dark spot belonged to the reticular pattern and had similar characteristics to the prototype. Olive tree candidates were located by computing the closed contours of the image through the Canny operator [38] and the centroid of each shape through the Chamfer Distance Transform [39]. The previous step is prone to produce many false positives, i.e., objects identified as olive trees because of the similar shape when viewed from above. This issue is perhaps the main limitation of tree detection methods that rely solely on the object's shape. For this reason, the authors exploited the typical arrangement of trees in olive groves according to a reticular structure in which each tree forms a precise angle with its neighbors. The detection accuracy resulting in this work was 98%.

Ozen and Bolca [40] compared four methods for olive tree counting in three distinct areas using Quickbird imagery: OLICOUNT, M-OLICOUNT, a template method, and the Geographic Object-Based Image Analysis (GEOBIA) approach implemented in the eCognition software (Trimble GeoSpatial, Munich, Germany). M-OLICOUNT is a modified version of OLICOUNT and includes the changes introduced to use multiple bands in its tree training module. Results showed that the template counting method had a higher accuracy where the topography was inclined and natural vegetation was mixed with olive trees. Other software methods showed better performance regarding time and costs in olive groves lying flat or slightly sloping areas.

Some challenges to overcome include distinguishing species with spectral similarities, discriminating between desired and invasive species, and species that are difficult to detect in high-density environments with narrow spaces between rows and tree canopies touching each other. Other difficulties regard mapping canopy edges due to conflicts between shade and illumination or the presence of ground vegetation [41–44]. New studies on this topic aim to achieve higher accuracy and capability in dealing with such problems. The goal is to test the approaches by implementing the methods in different conditions of plantations, sensors, flight altitudes, viewing angles, spatial and spectral divergences, and phenological phases, and trying to standardize the results obtainable. The use of multispectral (MS) sensors provides the advantage of using the near infrared (NIR) band, which is the most sensitive band for mapping canopy properties of vegetation [45]. Some features are distinctive enough to be detected in a panchromatic or single-band image. However, the difference in the spectral signature of different surfaces usually allows subtle variations to be noticed and, thus, detailed identification [45]. In this regard, the use of multiple bands for canopy identification allows for overcoming the limitations highlighted in the detection based only on the trees' shape, size, and spatial pattern [11,15]. This was shown by Daliakopoulos et al. [21], who proposed the use of the algorithm Arbor Crown Enumeration (ACE) on Quickbird imagery based on the combination of three procedures: blobs detection, Red band, and Normalized Difference Vegetation Index (NDVI) [46] thresholding. If applied individually, each procedure does not produce satisfactory results. Blob detection identifies all blob-like surfaces regardless if they represent trees' canopies, rocks, or other objects, leading to overestimations, especially in mixed land-uses imagery. Red band thresholding usually tends to clump tree canopies where the vegetation is denser,

causing an underestimation. The Red band depends on the reflection values with which the method was calibrated. NDVI thresholding is sensitive to the different characteristics unique to each image. ACE has as its strength that it can exploit MS images that carry more information than a single band. The combination of the three procedures improved the results obtainable from using singles by compensating for the limits of each. Indeed, the results showed differences do not hinder the tree canopy size or tree density performance due to blob detection.

García Torres et al. [20] described and exploited the algorithm Clustering Assessment (CLUAS, an add-on of the software suite ENVI), aimed at the automatic quantitative assessment of olive orchard's agronomic and environmental indicators. Quickbird satellite images and airborne MS imagery coupled with a supervised classification were used in the first stage. From the MS aerial photography, the bands Green and NIR were selected together with some indices (Blue, Green, Red, and NIR)/4, NDVI, and Ratio Vegetation Index (RVI) [47] for olive grove image assessment. Results showed the capability of CLUAS to provide the total number of clusters/olive trees, the whole surface of olive trees, the percentage of olive tree surface over the total, and the potential overall productivity.

Sarabia et al. [4] proposed a methodology for automatically counting olive trees in intensive orchards from MS UAV imagery exploiting digital surface model (DSM) information. The MS images were processed to generate a DSM which was converted into a greyscale image, where elevation information was approached as grey level values. The tree counting procedure was applied to the binary map obtained using the Otsu method and was focused on the analysis of the morphology of the connected segmented components in cases of overlapping of two crowns within rows. Elevation data were used for separating olive trees from the bare soil to obtain an image segmented into two classes. The results showed this method correctly detected trees with an accuracy of about 99%. The methodology was tested in an intensive olive grove of about 18 ha, showing its effectiveness in a complex scenario characterized by intra-row tree aggregations and a strong ground elevation variability. Providing rapid and reliable methods functional in both simple and complex scenarios is also highlighted in [43,48,49].

Karydas et al. [48] proposed a quick and easy semi-automated classification for mapping olive plantations on a sub-tree scale using GEOBIA on MS UAV imagery and based on a binary map (i.e., containing the two classes "Olive trees" and "Other"). A region-growing segmentation algorithm, the Multiresolution Segmentation algorithm (MRS) [50], implemented in the eCognition suite, was applied for the image segmentation. According to a trial-and-error procedure, the segmentation parameters were chosen. As stated by Hay et al. [51], the real challenge is defining appropriate segmentation parameters (typically based on spectral homogeneity, size, or both) for image objects of varying sizes, shapes, and spatial distribution that make up a scene so that segments can be generated to meet user requirements [52]. In tree detection, segmentation allows isolating the objects of interest, i.e., the tree crowns (or canopies) from the rest of the image or rather from the background data represented by the soil. Trees were segmented out of the background by exploiting thresholding values or using morphological operations of opening and closing, region growing, edge detection, and clustering [29]. Olive groves were previously divided into subsets based on dimensional and geometric properties of the trees, such as density, size, shape, and structure observed on the field. The choice of classifying individual internally segmented canopies gives the possibility, by applying VIs such as NDVI, to reveal extreme values of indices linked to known stress conditions. Similarly, Modica et al. [43] implemented a semi-automatic workflow to process MS UAV imagery for detecting and extracting olive and citrus trees' canopies with the final production of vigor maps (Figure 4). The three study sites tested were heterogeneous regarding tree plantation distances, crop management, crop composition, tree age, height, and crown diameters. In two of the study sites, the olive trees were present in an olive grove and a windbreak in a citrus grove. The authors proposed a GEOBIA unsupervised classification approach, implemented in the software eCognition Developer, consisting of an MRS segmentation of the UAV MS image and

subsequent classification of trees based on VIs (NDVI, SAVI, and Chlorophyll Vegetation Index—CVI) and digital surface models (DSM and Canopy Height Model, CHM).

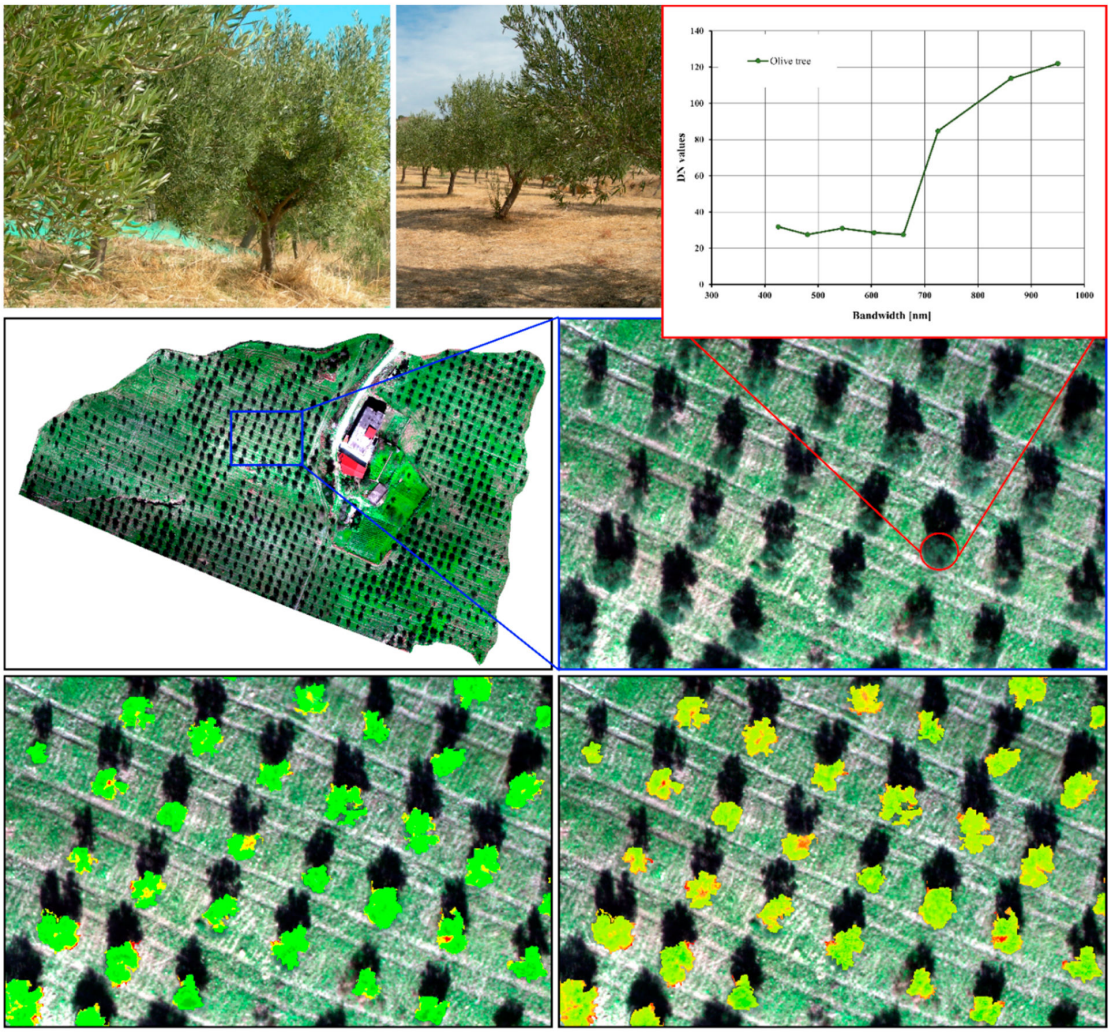

Figure 4. Top left and right respectively show olive trees and the spectral signature of an olive tree canopy. Bottom left and right photos, respectively, show applications of vegetation indices (VIs) Normalized Difference Vegetation Index (NDVI) and Normalized Difference Red Edge Index (NDRE) on olive tree canopies. Images were derived from a dataset used in [43].

Olive and citrus trees were classified by assigning a class to an object which fell within one or more chosen conditions, also called rules, based on values attributed to features as threshold values of VIs and topographic data. The use of DSM and CHM contributing to the distinction of different tree species, or simply separating tree crowns from the spectrally similar vegetation that covered the ground, improved the results obtained (ranging between 0.85 and 0.90 using the F-score accuracy parameter).

Solano et al. [49] implemented a GEOBIA semi-automatic workflow for olive tree detection and extraction, testing the reliability of WorldView-3 satellite imagery and deriving some VIs to analyze olive trees' vegetative vigor: NDVI, Normalized Difference Red Edge Index (NDRE) [53], Modified Soil Adjusted Vegetation Index 2 (MSAVI 2) [54,55], Modified Chlorophyll Absorption Ratio Index Improved (MCARI2) [56], and NDVI 2 [57–59].

The study sites tested were different: the first olive grove suffered various diseases, which reduced its development, while the second was well managed. The GEOBIA approach was implemented in the Imagine object of the Erdas Imagine suite (Hexagon Geospatial, Madison, WI, USA) as a semi-automatic process to extract single olive tree

canopies and eliminate the spectral disturbances of soil background. The results, showing an overall accuracy in tree extraction of about 96%, demonstrated the reliability of WorldView-3 data relying on high spectral, radiometric, and spatial resolution.

In the last decade, machine learning algorithms attracted much attention in the RS research framework [60], demonstrating their effectiveness in mapping crops [61] and weeds [41,62], disease detection [63,64], and land cover assessment [65–69]. An example of the application of machine learning supervised algorithms for olive tree detection is given by Waleed et al. [25], which combined pre-processing, segmentation, feature extraction, and classification techniques. The pre-processing step provided for eliminating noise. It was followed by segmentation using the K-means clustering algorithm. Several supervised machine learning algorithms were tested: Naive Bayes (NB) [67,70,71], Support Vector Machine (SVM) [72,73], Multi-layer Perceptrons, and Random Forest (RF) [74]. Results showed RF outperforming other algorithms with an overall accuracy of 97.5%.

Modica et al. [42] compared the performance of three different GEOBIA approaches based on four machine learning algorithms: K-Nearest Neighbour (KNN), SVM, RF, and NB. In particular, a supervised classification of MS UAV imagery was carried out in three different software suites: Orfeo ToolBox (OTB, www.orfeo-toolbox.org (accessed on 14 March 2022)) [75], Scikit-learn [76,77] and eCognition Developer. As for olive tree class, the highest value of accuracies was reached by SVM performed on eCognition with about 96% of F-score.

Castillejo-González [78] mapped olive trees using Quickbird's pan sharpened images and evaluated pixel- and object-based classification approaches through the comparison of four classification algorithms: Minimum Distance (MD), Spectral Angle Mapper (SAM), Maximum Likelihood (ML) and Decision Tree (DT). Results showed ML and DT were the two most precise classifiers and that greater weight given to the Red and NIR bands in the pan sharpening process increases the accuracy of canopy delineation. No difference was observed between pixel-based and object-based analyses. However, Lu and Weng [79] highlighted that the object-based classification approaches demonstrated better performance than pixel-based approaches in mapping individual landscape features. Also, Šiljeg et al. [80] tested ML and SVM classification algorithms within pixel-based and GEOBIA-based classification approaches for mapping olive trees in UAV imagery. Results showed SVM algorithm performed better in both approaches and particularly more accurately in the GEOBIA approach reducing shadow problems.

Peters et al. [81] demonstrated the usefulness of combining different types of information and data in olive tree detection. VHR imagery and synthetic aperture radar (SAR) data were used for implementing an object-based classification to map olive groves by integrating data from different sensors: multispectral Airborne Digital Sensor (ADS40), Radar Aeroporte Multispectral d'Etude des Signatures (RAMSES SAR) and TerraSAR-X. The processing chain for object-based olive grove mapping was followed: the multi resolution segmentation algorithm was used for defining objects, features calculation was executed for each object (shape, texture, spectral reflectance in optical imagery, and backscattering in SAR imagery), training and validation of the classifier used, and RF. Results showed that although SAR imagery alone did not contribute to the production of satisfying olive maps, its combination with MS imagery increased the mapping accuracy of RF to 90.5%. Also, Akcay et al. [82] investigated the combined use of MS and SAR satellite imagery to detect olive trees. The authors used Sentinel-1's and Sentinel-2's free multi-temporal/multi-sensor images. They used data acquired between the dates from April 2017 to May 2018, freely downloaded from the Copernicus Open Access Hub [83]. Different combinations of SAR, MS, and NDVI data were stacked, and supervised classification based on the RF algorithm was tested. The combinations were Sentinel-1–Sentinel-2, Sentinel-1—NDVI, and Sentinel-2—NDVI. Results showed that dual data fusion of Sentinel-1–Sentinel-2, Sentinel-1—NDVI, and Sentinel-2—NDVI gave an overall accuracy of 73.33%. In particular, the addition of NDVI to Sentinel-1 and Sentinel-2 data positively affected accuracy.

The alternative to counting trees before image post-processing was demonstrated by Salamí et al. [31], who proposed a method for counting olive trees in real-time during UAV (RGB) flight. This process involved the segmentation of each image (the two techniques, color-based and stereo vision-based segmentation algorithms, were tested), geolocation of each tree, and image overlay corrections. The embedded computer on the UAV processed the images on-the-fly, and sent the relevant findings, such as the geographic coordinates of each tree, to the ground station. Therefore, the results can be visualized in real-time at the ground station. Such a method, combined with existing cloud services, would allow end-users to have rapid access to user-friendly data without needing specific software, using only the browser. Results showed a capacity to classify trees with an accuracy of 99%.

In recent years, deep learning (DL) techniques have grown in popularity in RS application in agriculture, among which include weeds detection [84], crop classification [85], and tree detection, as shown in [32,86–88]. Applications of DL for the detection of olive trees are also very recent. Ye et al. [24] tested low-cost UAV (RGB) imagery in the semantic segmentation model U2-Net for olive tree crown extraction. U2-Net was compared to other DL models. Despite the positive results obtained, the model showed some limits. The first limit derives from the camera used to investigate only the visible, making it difficult to distinguish different vegetation that shares a similar spectrum. Other limits are the presence of several "vertices" and crowns belonging to the same tree, and the presence of adjacent crowns very close together, according to the density of the planting scheme. Lin et al. [89] used DL to map olive groves in two regions of Morocco, one semi-arid and the other sub-humid, comparing the effectiveness of high-resolution imagery, PlanetScope 3-m MS imagery, and VHR imagery and WorldView-2 and WorldView-3 RGB imagery with 0.5/0.3-m of spatial resolution. Images were acquired for the years 2018–2019. The objective was to test the model generalizability under different levels of spatial variability. Results showed that VHR imagery had better performances in capturing the texture feature of olive groves in both sub-humid and semi-arid regions. In contrast, PlanetScope imagery could only detect olive groves with larger canopy sizes and smaller tree spacings. The temporal information was not helpful for mapping using PlanetScope images of young, smaller, and more spaced olive groves in the semi-arid region. At the same time, the result was better in mapping olive trees in a sub-humid region where older trees had prominent texture features.

Table 1 below summarizes the research focused on tree detection and counting. This is the topic with the largest number of articles identified which, moreover, collectively covered the use of different RS platforms (satellites, aircraft, and UAVs) and the different types of sensors, from those producing PAN and RGB images to MS and SAR.

Table 1. References dealing with olive trees detection and counting. The remote sensing (RS) platform used, the type of sensor and the main objectives of the researches are also indicated.

Reference	Platform	Sensor Type Used *	Aim of the Study
[82]	Satellites Sentinel-1 and Sentinel-2	SAR and MS	Combining multi-sensor optical and SAR satellite images for tree detection
[11]	Aircraft - *	RGB	Morphological Recognition of Olive Grove Patterns
[22]	Satellite IKONOS	-	Tree detection and counting
[78]	Satellite Quickbird	MS	Evaluating four supervised classification algorithms, applied to pixel- and object-based classifications, for tree detection
[21]	Satellite Quickbird	MS	Tree detection and counting
[20]	Aircraft CESSNA 421	Airborne KODAK (MS)	Automatic assessment of quantitative agronomic and environmental indicators
	Satellite Quickbird	MS	
[19]	Satellite Quickbird	PAN	Tree detection and counting

Table 1. *Cont.*

Reference	Platform	Sensor Type Used *	Aim of the Study
[29]	Satellite Quickbird	RGB	Tree detection and counting
[16]	Satellite SPOT 5	PAN	Testing new texture segmentation scheme for vegetation extraction
[15]	Satellites Quickbird and IKONOS	PAN	Tree detection
[18]	Satellite IKONOS	PAN	Improving edge detection and watershed segmentation with anisotropic diffusion and morphological levellings
[48]	UAV eBee	multiSPEC 4C (MS)	Tree detection
[89]	Satellite PlanetScope	MS	Tree detection using Deep Learning on high resolution and very high-resolution satellite imagery
	Satellite WorldView-2 and 3	RGB	
[12]	Aircraft -	ADS40 camera RGB	Tree detection and counting
	Satellites Quickbird and IKONOS	PAN MS	
[43]	UAV Multirotor G4 Surveying-Robot	Tetracam μ-MCA06 (MS)	Tree detection and monitoring
[42]	UAV Multirotor G4 Surveying-Robot	Tetracam μ-MCA06 (MS)	Comparing the performance of three different GEOBIA * approaches based on four machine learning algorithms
[13]	Satellite Quickbird	PAN	Tree detection and counting
[40]	Satellite Quickbird	MS	Comparing tree detection and counting methods
[81]	RAMSES SAR and TerraSAR-X satellites	SAR	Mapping olive groves using VHR * optical and radar imagery
	Aircraft -	ADS40	
[17]	Aircraft -	-	Localising missing plants
[31]	UAV DJI Phantom 4	RGB	Real time tree counting method using UAV
[4]	UAV DJI Matrice 100	MicaSense RedEdge-M (MS)	Tree detection and counting
[80]	UAV DJI Matrice 210 RTKV2	Zenmuse X7 (RGB)	Analysis of UAV imagery applicability and Comparison of algorithms in pixel-based and GEOBIA classification approaches for tree detection
	UAV DJI Matrice 600 Pro	MicaSense RedEdge-MX (MS)	
[49]	Satellite Worldview-3	PAN-MS	Tree detection and monitoring
[30]	Satellite Quickbird	Red	Tree detection and counting
[25]	Satellite -	RGB	Tree detection
[24]	UAV DJI Phantom 4	RGB	Tree detection using UAV combined with U2-Net Deep Learning model

* PAN = panchromatic; * MS = multispectral; * RGB = red-green-blue; * SAR = synthetic aperture radar; * - = missing information; * GEOBIA = geographic object-based image analysis; * VHR = very high resolution.

3. Pruning

Pruning in olive growing brings several benefits: in young trees, it is performed to give an adequate structure for future production while optimizing the exposure of the canopy to the sunlight and maintaining the equilibrium between vegetative and reproductive functions [90,91]. Proper pruning can help ensure adequate canopy illumination by providing sufficient exposure to the canopy's innermost leaves through a good number of thinning cuts and a spatially balanced distribution of vegetation [27]. As stated by Michalopoulos et al. [3], pruning techniques should focus primarily on improving light distribution

within the canopy (photosynthesis oriented), foliage aeration, and good development of bearing shoots [92]. Considering these assumptions, pruning is linked to production, as the objective is to maintain the actual yield as close as possible to the potential yield [93]. It should not be forgotten that pruning depends and is carried out differently with all that follows at the operational and economic level, depending on the type of olive grove and the biophysical characteristics of the cultivar. Therefore, in this perspective, carrying out the planting, choosing the proper cultivar, and the configuration of the plant is a very delicate decision, both for the high degree of irreversibility that it involves both for the leading role it plays in the economic success of the olive grove. It is, in particular, to combine the best density of planting (number of plants/ha), planting system (geometric arrangement of plants in the field), and form of farming (distribution in space given to the permanent and productive structures of the plant). In Mediterranean areas, due to lower rainfall and the long period of summer drought, there is a tendency to keep the planting density low in order not to run into problems of water stress, which is frequent when the leaf area per unit of the soil surface is quite high [27]. This has helped increase the value of dry lands and marginal lands in the recent past and enhanced the value of local cultivars. Large trees characterize the traditional plantings, 100–300 trees/ha mainly arranged in squares (with tree distances of 5–7 × 6–8 m) and crowns that very frequently exceed 4–5 m in height and 130–150 m^3 in volume [27]. In the traditional olive groves, the operations of pruning and harvesting, which are difficult to mechanize, are made complicated by the location of olive groves in marginal areas and on slopes and, of course, the large size reachable by the trees [94,95].

Intensive plantings are characterized by planting densities of 300–1000 trees/ha [96]. They can be distinguished as low-density olive groves with trees arranged in squares at a distance of 5–7 m × 5–7 m, with a height of about 4 m and 50 m^3 in volume for each plant. Medium-density plantations have a higher number of trees, 500 plants/ha, while high-density plantations reach 800 plants/ha [27]. In these plantings, harvesting can be mechanized, while pruning can be manually done by using hacksaws mounted on telescopic rods [97].

Super-intensive plantings are characterized by a very high planting density (1100–2500 trees/ha) [98] with distances of 3.5–4 m between rows and 1.2–1.6 m on the row. Normally, they are composed of cultivars with relatively contained development in order to obtain relatively high productions starting from the third year after planting, and make pruning and harvesting operations fully mechanized and continuous along the rows [96,99–101]. Therefore the super-intensive systems are not suitable for olive growing practiced in an agronomic context characterized by hills, sloping lands, and small farms and in general in conditions of reduced availability of water as in some Mediterranean countries such as Italy and Greece [27,100].

Despite its importance, pruning remains an expensive practice, mainly when performed manually [102]. In fact, it requires experienced operators, often in short supply in the main production areas, driving up costs [93]. That is why a cheaper and less labor-intensive technique is needed [103]. One solution may be implementing mechanical pruning to increase adequate field capacity and reduce costs [97]. This practice is widespread in super-intensive olive groves, while light manual pruning is recommended in small olive groves [96,104]. It is important to keep tree and crown base height within a defined range to facilitate crop access [105]. Therefore knowledge of canopy sizes, tree heights, and base canopy heights enables efficient planning and management of production [106] and facilitates mechanization of operations, especially during the harvesting [96]. Harvesting performance is positively influenced by an olive grove whose architecture is well adapted to the harvesting system [90,91,107]. Pruning should be done in relation to the harvesting, considering that the pruning for manual harvested olive trees should be different from mechanical harvested ones [93]. In the case of mechanical harvesting in intensive and super-intensive groves, each harvester requires specific pruning to achieve high efficiency. Investigations into the effects of pruning generally involve characterizing

the tree's architecture by measuring the tree's primary dimensions, such as its height, and estimating canopy area and volume using appropriate equations [108]. However, this work being laborious and the canopies irregularly shaped, it is difficult to achieve accurate results using this approach. In addition, methods involving ground measurements cannot be used in large groves [106]. In this case, the RS platforms such as aircraft and UAVs can be used for collecting olive trees' dimensional data.

Jiménez-Brenes et al. [108] developed an automatic GEOBIA method for identifying olive trees and computing their primary 3D dimensions from UAV imagery: height, projected area, and crown volume. The study field was divided into three subsets by distinguishing olive trees differently pruned to quantify pruning impact: traditional, adapted, and mechanical treatments. The GEOBIA approach, developed using RGB images and DSM, provided for distinguishing tree crowns from the bare soil below. Finally, an automatic procedure allowed for identifying each tree's position, height, projected area, and crown volume. Other research has included aerial LiDAR (light detection and ranging) sensors [106,109], commonly used for estimating tree heights, crown base, crown volume, stem diameter, and volume in forestry [110]. Hadas and Estornell [109] evaluated the accuracy of automatically determined tree geometric parameters (tree height, crown base height, crown diameters, crown area) based on the density of LiDAR data. However, results also showed that similar results could be obtained, in terms of tree height and crown base height, either by using sparse or dense LiDAR data. Generally, it was demonstrated that the accuracy of estimating geometric parameters is independent of tree size. In another research, Hadas et al. [106] proposed a method for estimating trees' geometric parameters (tree height, crown base height and crown diameters), which exploited the canopy's point cloud produced by an airborne LiDAR. The methodology is based on the α-shape algorithm [111], which describes the shape of a finite set of points on a plane delineating the boundaries of objects (tree crowns in this case), represented by a group of points having heterogeneous distribution and low density. The authors compared tree dendrometric parameters (tree height, crown base height, length of the longer diameter, and perpendicular diameter) estimated from airborne LiDAR with field measurements to assess the quality of an automatic approach combined alpha-shape algorithms and principal component analysis (PCA).

Recycling residual biomass obtained from tree pruning has become a common practice due to the possibility of using it as a feedstock for biofuel production. An alternative involves using olive pruning residues to cover the soil and improve fertility [112]. Using LiDAR sensors, RS for biomass pruning estimation provides an alternative to time-consuming and expensive field measurements. An example is given by Estornell et al. [105], which used airborne LiDAR technology of low pulse density points to quantify olive trees' height and volume. The same authors [113] developed non-destructive methods based on LiDAR data for evaluating and quantifying pruning residual biomass. In the research mentioned above, several variables were analyzed to estimate pruning biomass: dendrometic variables derived from field measurements; dendrometric variables derived from LiDAR data; variables obtained from the distribution of the height and intensity of LiDAR data in each olive tree. In particular, field data provided trunk diameter, total height, crown height, and mean crown diameter. After performing the measurements, each tree was lightly pruned and the residues weighed. The data derived from LiDAR provided better results for estimating direct and indirect parameters, i.e., area and pruning biomass, than those obtained by field measurements.

Table 2 below summarizes the researches about pruning that involved the use of RS platforms and sensors. As the table shows, of the five reviewed, as many as four involved the use of LiDAR sensors from aircraft.

Table 2. References dealing with pruning. The remote sensing (RS) platform used, the type of sensor and the main objectives of the researches are also indicated.

Reference	Platform	Sensor Type Used *	Aim of the Study
[105]	Aircraft - *	LiDAR—Leica ALS60 sensor	Quantifying the height and volume of olive trees
[113]	Aircraft -	LiDAR—Leica ALS60 sensor	Quantifying pruning residual biomass
[109]	Aircraft -	LiDAR—Leica ALS60 LiDAR—Leica ALS50-II	Computation of tree height, crown base height, crown diameters, crown area
[106]	Aircraft -	LiDAR -	Computation of tree height, crown base height and crown diameters
[108]	UAV MD4-1000	Olympus PEN E-PM1 (RGB)	Tree detection and computation of position, projected canopy area, canopy height and volume

* LiDAR = light detection and ranging; * - = missing information; * RGB = red-green-blue.

4. Yield

Olive growing's profitability is determined by yield, which in turn depends on the grove category [96]. The correct design of the olive grove in orientation, row height and width, alley width, etc., is important for maximizing light interception and productivity [114]. The availability of new planting systems and the introduction of more efficient management strategies contributed to spreading olive growing outside of traditional cultivation areas [115]. Regarding the production and yield of different planting systems, trials under both rain fed and irrigated conditions carried out in low-density olive groves showed higher production at tree level, while higher yield per hectare was obtained in high-density olive groves [116,117]. Planting density affects the size of individual trees in both trunk and canopy sizes, as reported in [118]. Tree size increases under low-density conditions, while an opposite effect is obtained in high-density olive groves [96]. Canopy size and shape also affect olive trees' fruiting potential [104,119]. In addition, productivity depends on other factors, including soil fertility, management practices, climate, and meteorology [120].

The development of reliable methods for yield prediction can be very useful for farmers in managing (spatially and temporally) cultivation techniques such as irrigation and fertilization in particular areas or trees characterized by lower yields [121,122]. Conventional olive yield assessment methods based on ground surveys are time-consuming, expensive, and inaccurate. RS technologies can support the production forecast [123]. For yield forecasting, predicting phenological phases is a valuable tool, as shown in several studies (Table 3). However, satellite or proximal surveys and ground surveys are unlikely to effectively provide information on the seasonal patterns of phenological events due to the different scales of observation. In this regard, statistical models based on meteorological parameters represent a potential solution to combine ground-based phenological observations and those provided by satellite-derived VIs [124,125]. Machine learning techniques already applied to crop yield optimization and plant phenology forecasting can improve the accuracy of phenological models [126,127]. Azpiroz et al. [128] developed a phenology prediction model based on climate and geophysical data. Three datasets were used to calculate predictors for the phenological phases of the olive tree: the weather registry obtained from the open-access ERA5 dataset (Copernicus Climate Change Service, 2017); satellite dataset (ALOS Landform) providing geophysical input data, i.e., latitude and longitude of the olive groves, and the slope; MODIS, providing surface spectral reflectance data.

Maselli et al. [120] developed and tested a multi-step methodology integrating RS and ancillary data to estimate spatial and temporal variations of olive yield within a decade (2000–2009) in Tuscany (Italy). In particular, IKONOS, ETM+ high-resolution imagery and MODIS NDVI were used, while ancillary data included daily temperatures and precipitation for the decade examined, the geographical distribution of olive groves (CORINE land cover), soil feature data, and a digital terrain model (DTM). The data combined within a modified parametric model (C-Fix) [129] allowed the prediction of daily olive tree gross primary production (GPP). GPP is then combined with respiration estimates

from a biogeochemical model (BIOME-BGC) [130] to simulate the net primary production (NPP), which was finally converted into yield. Similarly, Brilli et al. [131] developed a multi-step methodology for estimating olive grove GPP by modeling it in a complex agricultural context, simulating the behavior of both primary ecosystem components: ground vegetation and olive trees, separately. Daily temperatures and precipitation for the two years examined (2010–2011) were obtained from ancillary sensors linked to the eddy covariance station, while RS imagery derived from IKONOS, ETM+ together with multi temporal NDVI values from MODIS. GPP was estimated using the C-Fix model, and the modeling performances were compared with GPP data derived from eddy covariance measurements.

Kölle et al. [132] proposed a method to assess compensation from an insurance based on yield losses in olive growing by using satellite-based weather meteorological indices. The authors, presenting a case study in Andalusia (region of Spain), investigated which phases of the satellite-based vegetation health indices have the highest relationship with olive oil yields. Some indices were tested on MODIS' imagery: the Vegetation Condition Index (VCI), the Temperature Condition Index (TCI) and the Vegetation Health Index (VHI). Meteorological indices for temperature and precipitation are used as benchmarks. Results showed that the relationship between olive oil yields and the indices is more pronounced for inflorescence development, flowering, fruit growth, and oil accumulation stages. Sola-Guirado et al. [133] evaluated olive annual yield forecast based on tree canopy measurements. In particular, they proposed relating trees' manually measured canopy volume to their crown area obtained from UAV (RGB) imagery for producing yield thematic maps for all olive grove categories (except super-intensive groves). In particular, manual (or ground) measurements and UAV data were taken by selecting random trees from olive groves irrigated intensive, irrigated traditional, and rain fed traditional. Stateras and Kalivas [123] assessed olive trees' geometrical characteristics (height, area, and canopy volume) in non-linear hilly olive groves to develop a yield forecast model using MS UAV imagery. Tree crowns were isolated and classified using GEOBIA calculating the area of the tree canopy, the mean, the minimum and the maximum height, NDVI, and the slope for each of them. Each of these variables was tested to verify the correlation with the yield. The mean NDVI of the tree canopy, canopy volume, and the average slope in correspondence to each tree were used to implement a yield forecasting model. This model can be used in Mediterranean regions (such as Greece), where hilly non-linear olive tree groves represent a common way of cultivation.

Ortenzi et al. [134] aimed at obtaining an approximate early production estimation of olive groves based on the canopy radius extracted from UAV (RGB) imagery. The surveyed groves were divided into four plots, three of which were training plots and one as a test plot. In each plot, they assessed the leaf surface segmenting imagery and counted the pixels belonging to the canopy (classified using KNN supervised learning algorithm), automatically deriving the canopy radius. The olive production per tree was measured at harvesting and modeled as a function of canopy radius. Methodologies such as the one proposed by the authors could help farmers track the amount of production by field area, identify any problems, or define a production and marketing strategy in advance.

Table 3 below summarizes the researches on yield monitoring that involved the use of RS platforms and sensors.

Table 3. References dealing with the monitoring of yield. The remote sensing (RS) platform used, the type of sensor and the main objectives of the researches are also indicated.

Reference	Platform	Sensor Type Used *	Aim of the Study
[128]	Satellite Terra (EOS AM-1)	MODIS (MS)	Phenology prediction
[131]	Satellites IKONOS—Landsat 7- MODIS	MS	Simulation of olive grove gross primary production
[132]	Satellite Terra (EOS AM-1)	MODIS (TH)	Estimation of yield dependence on extreme weather conditions
[120]	Satellites IKONOS—Landsat 7- MODIS Aircraft - *	MS	Simulation model of olive fruit yield
[134]	UAV DJ SPARK	- (RGB)	Early production estimation
[133]	UAV DJI S800	Sony NEX7(RGB)	Yield forecast
[123]	UAV DJI Matrice 100	Parrot Sequoia (MS)	Yield forecast

* MS = multispectral; * TH = thermal; * - = missing information; * RGB = red-green-blue.

5. Phenotyping and Monitoring of Trees' Biophysical Parameters

Crop phenotyping can be defined as the monitoring of morphological, physiological, and biochemical traits which result from the interaction between genetic and environmental factors [115,135]. The preferred agronomic traits in olive growing are those related to the earliness of production, high productivity and oil quality, and resistance to abiotic and biotic stresses [136–138]. Some characteristics of olive trees related to geometrical canopy measures, vegetative growth habits, and vigor are important in phenotyping trials because they are linked to aspects of management, such as the form of training, plantation pattern to be adopted, pruning, and harvesting [6,137,139–141]. Also, qualitative parameters of fruits and oil depend on the geometry of the foliage, its shape, and size, as it affects the penetration of sunlight in the canopy and its distribution [142]. High variability in selection crosses together to the long juvenile period of the olive tree, making it complex, lengthy, and expensive to find a genotype with all desirable traits (productivity, high oil quality, and diseases and pests) [143].

Traditional methods used in the field for collecting phenotypic data require experience and are time-consuming [115,137,144]. The manual measurement of the geometrical characteristics to estimate the area and volume of the canopy using empirical models generates results that are inconsistent both for human errors in the field and for model errors when the canopy is assimilated to a regular polygon or a spheroid [145,146]. In this framework, the use of UAVs responds to the need to speed up and reduce costs thanks to their flexibility and high spatial, spectral, and temporal resolutions [135,144,147]. Several research efforts have focused on the use of UAVs in olive phenotyping [115,137,140,143,145,148,149]. Gómez-Gálvez et al. [137] calculated canopy traits measurements in different olive cultivars by comparing UAV with conventional ground measurements. In particular, in each tree, crown length radius, crown width radius, crown height radius, and tree height were measured. A further objective was to demonstrate the usefulness of UAV measurements for identifying differences between cultivars and olive trees of different ages within the same cultivar. Avola et al. [149] tested some VIs obtained from MS UAV data and exploited them to discriminate olive cultivars with different scion/rootstock combinations. Data were processed through different statistical approaches, univariate (ANOVA) and multivariate (principal components analysis, PCA, and linear discriminant analysis, LDA). Results showed the efficacy of seven VIs (NDVI, Simple ratio SR [150], Green normalized difference vegetation index GNDVI [151], Green red normalized difference vegetation index GRNDVI [152], Simple ratio NIR green vegetation index GRVI [153], Normalized difference green/red difference vegetation index NGRDI [154], and RVI [155] in scion recognition while unsatisfactory results were obtained for discrimination between root-

stocks. Torres-Sánchez et al. [143] research focused on quantifying the dwarfing effect of different rootstocks in 'Picual' olive cultivar by using UAV photogrammetry to select the more suitable cultivar for super-intensive training systems. Generation of the 3D point cloud from UAV imagery and GEOBIA algorithm was used to measure canopy height, projected and cross-sectional canopy areas, and canopy volume of olive trees derived from different rootstock-scion combinations [156].

One of the phenotyping's objectives in olive growing is focused on finding key traits of cultivars best suited to super-intensive (hedgerow) training system (continuous canopy with a width less than 1–1.5 m), particularly adapted to fully mechanized harvesting, easy pest and disease control, and high productivity [156]. Selection of these cultivars has focused on characteristics such as early and abundant fructification obtained 3–4 years after planting and production stability with reduction of alternation, possibility to mechanize completely and continuously pruning and harvesting thanks to cultivars of low vigor dwarfing rootstocks with a compact habit of growth [27,96,157]. Given the importance of this issue for modern olive growing, several pieces of research have involved monitoring super-intensive olive groves and in the framework of breeding trials. Caruso et al. [115] evaluated the ability of MS UAVs imagery to detect differences in geometrical (canopy height, projected canopy area, and volume) and spectral canopy characteristics in a super-intensive olive grove. Furthermore, a good relationship was demonstrated between the pruning mass material weighted on the ground and its volume estimated by UAV images. De Castro et al. [148] developed and tested a UAV-based high-throughput system in olive breeding applied on very young olive trees of which the architectural features are monitored in two training systems (intensive and super-intensive). The authors, after configuring UAV flight altitude and image overlapping, developed a GEOBIA algorithm to generate key agronomical traits considered in olive phenotyping useful for selecting the best genotypes: canopy height, canopy area, and canopy volume.

Rallo et al. [140] evaluated the validity of using a UAV-based methodology to estimate multi-temporal architectural features of olive canopies in breeding trials aimed at selecting the most promising genotypes. The research links to the previous [148], in which an GEOBIA algorithm based on photogrammetric point clouds was used. Using this methodology, Rallo et al. classified and selected olive genotypes by analyzing four architectural parameters: canopy height, diameter, projected canopy area, and volume.

Díaz-Varela et al. [145] tested a low-cost UAV system for estimating olive crown parameters both on discontinuous canopy (open vase training form) and continuous canopy (hedgerow) groves in the framework of breeding trials. For this purpose, several image reconstructions using Structure from Motion (SfM) techniques on imagery with high overlap allowed the generation of detailed DSM and orthomosaic. Finally, the parameters canopy height and crown diameter were computed using geographical information system analyses and object-based classification.

Plant architecture is a crucial issue for the characterization and monitoring of olive trees' biophysical parameters [145]. Geometric characteristics of trees can be helpful in monitoring crop status and agronomic aspects related to production, fertilization, irrigation, pruning and pest management [158]. UAVs represent an alternative solution compared with manual measurements that is less time consuming and applicable on a large scale rather than just a few individual trees. UAVs fly at very low altitudes with large overlaps and different angles, providing hundreds of images at centimetric resolution from which DSMs can be generated [159], exploiting the automatic photo-reconstruction method based on the SfM technique [160]. Through the SfM deriving from the images acquired from multiple viewpoints, three-dimensional geometry of objects, olive trees, in this case, are constructed [137,161]. The DSM allows representing the irregular geometry of tree canopies providing detailed information on dimensions parameters such as tree height. Zarco-Tejada et al. [161] used very high-resolution imagery derived from low-cost UAV cameras and automatic DSM generation methods for tree height quantification in olive groves. Height ground measurements were compared with those carried out on DSM

using the identification of local maxima. In detail, the distance between DSM local maxima, represented by tree tops, and the minimum DSM value, represented by ground height, was measured and compared to ground truth measurements yielding a high correlation. This method proved effective in the presence of trees with open canopies that allowed a glimpse of the ground below. The accuracy of results depends on the UAV flight altitude and imagery overlapping. In this regard, Torres-Sánchez et al. [162] tested UAV imagery at flight altitudes of 50 and 100 m over two olive tree groves to generate DSMs representing the tree canopies. The objective was to evaluate the influence of different forward overlaps (from 58% to 97%) on computation time and accuracy of DSM, showing the configuration with 100 m flight altitude and forward overlap percentage is the best and a significant reduction in computation time. The importance of DSM in calculating the geometric parameters of the canopy is highlighted by Torres-Sánchez et al. [158]. Torres-Sánchez et al. proposed an automatic procedure for a high-throughput 3D monitoring of olive trees using UAV imagery and GEOBIA. From UAV imagery (mounting two types of sensors, RGB and MS), a DSM was derived and used as input data in the GEOBIA procedure. This procedure permits the classification of each tree exploiting two VIs, Excess Green (ExG, [163]) and NDVI, for RGB and MS imagery, respectively. For each tree, its position and its geometric features (canopy area, tree height and canopy volume) were calculated. The local maxima (tree-top) and minima pixel (ground baseline) were exploited by the GEOBIA algorithm for calculating trees' height while canopy volume was obtained by multiplying the height and area of each tree pixel.

Caruso et al. [164] confirmed that MS UAV imagery and SfM techniques allow for estimating biophysical and geometrical parameters. Tree height, canopy diameter, and volume of olive trees were measured based on DSM and DTM. The height was calculated by exploiting the average height of the terrain surrounding each tree and the maximum height of every tree. The diameter was calculated by exploiting the circularity of the tree surface view from above. Lastly, leaf area index (LAI) direct measurements significantly correlated with NDVI, as shown in [14]. Berni et al. [14] combined two types of sensor, MS and thermal, mounted on UAVs. Among the estimated biophysical parameters, LAI and chlorophyll content were measured in an olive grove. Three VIs were calculated from UAV imagery: NDVI for assessing the estimation of canopy LAI; the physiological reflectance index (PRI) [165], developed for xanthophyll cycle pigment change detection, was exploited to assess its capability for water stress detection; the index TCARI/OSAVI obtained from the ratio of transformed chlorophyll absorption in reflectance index (TCARI) [166] to the optimized soil-adjusted vegetation index (OSAVI) [167]. In particular, this ratio helped reduce soil background and LAI variation, providing predictive relationships for chlorophyll concentration estimation in closed crops [166] and open tree canopy groves [168]. Results showed NDVI was highly correlated with LAI field measurements. In addition, a high correlation between TCARI/OSAVI and chlorophyll content was shown.

Anifantis et al. [169] tested three different methods for evaluating the tree row volume (TRV) of a super-intensive olive grove by comparing UAV imagery 3D techniques with manual and traditional methods of TRV measurement. The first method consisted of producing a 3D model from UAV images, while the second involved manual measurement using an optical meter and a portable GNSS. The third method, adopted by Codis et al. [170], foresaw multiplying the average values of the height and thickness of the crown for each olive row, multiplied by the area of 1 ha and divided by the inter-row width. Results showed the reliability of data obtained by UAV imagery. Another example of volume calculation from 3D models was shown by Jurado et al. [159], who used RGB point cloud and MS UAV imagery for olive grove 3D reconstruction. Olive trees detected in the point cloud were segmented and classified using spatial and spectral features. VIs, NDVI, RVI, Green Ratio Vegetation Index (GRVI) [171], and NDRE were used for monitoring olive grove health status together with morphological data obtained from the 3D model, volume and height, with a view to a multi-temporal analysis of data obtained from two UAV flights one year apart.

In the evaluation of productivity, estimating the interception of radiation is important because biomass production is directly related to the intercepted radiation, and this also happens in olive tree canopies [172]. The work of Guillén-Climent [173] focused on estimating the fraction of Intercepted Photosynthetically Active Radiation (fIPAR) in an olive grove. Ground measurements included the interception of solar radiation of canopies (by means of a ceptometer), dimensional properties such as canopy height and crown width, and the LAI. A six-band MS camera mounted airborne was used for aerial imagery acquisitions. fIPAR's estimation was performed employing a couple of radiative transfer models: Forest Light Interaction Model which is a 3D model of light interaction with vegetation canopies (FLIGHT) [174] and a model of PAR interception by olive canopies called "Orchard Radiation Interception Model" (ORIM) already used for estimating the radiation intercepted by an olive grove at instantaneous and daily levels [172]. Both models permit assessing the estimation of instantaneous fIPAR through the simulation of planting grids, tree dimensions, and soil background effects, row orientation, tree dimensions, and slope of the field, allowing the generation of several 3D scenes for the assessment of the impact of the canopy architecture, crown structure, and biochemical inputs.

Focusing on the relationship between the processes of absorption, reflection, and transmission affecting vegetation and describing the interactions between incident radiation the biochemical constituents of leaves and the biophysical characteristics of the canopy, Noguera et al. [175] worked on assessing the nutritional status of olive crops. In particular, a method for the recovery of NPK (Nitrogen, Phosphorus, and Potassium) canopy content in olive trees by using MS UAV imagery under different fertirrigation treatment was developed. Different retrieval techniques partial least squares regression (PLSR), artificial neural network (ANN), support vector regression (SVR), and gaussian process regression (GPR) were tested for NPK leaf content estimation by exploiting data extracted from UAV imagery as input variables and the results of chemical analyses as reference. The results showed the best performance of the ANN approach.

To our best knowledge, there are only three studies involving the use of satellite imagery to calculate biophysical parameters of the canopy [176–178]. Gómez et al. [176] evaluated the potentialities of using airborne hyperspectral sensors and Quickbird satellite imagery for determining and mapping tree canopy size, canopy transmittance, and LAI of single olive trees. Tests were carried out in both traditional and intensive olive groves. The dimensional parameters of the canopy, area, and volume were measured. The projected canopy volume of each tree was calculated using the coordinates of the tree silhouette: the tree canopy was ideally divided into eight sectors obtained by eight equidistant trapezoids which were placed around the central-vertical axis of the olive tree. The volume was obtained by summarizing each trapezoid using the second Pappus-Guldinus theorem [179]. The projected canopy area was obtained, firstly marking the perimeter of the orthogonal projection of the tree canopy onto the soil surface using a pole in eight points, generating eight equidistant transects from the center of the tree. Finally, the canopy area was calculated by summing the areas of circular sectors for each transect. Abdelmoula et al. [178] used Sentinel-2 images for estimating olive biophysical parameters as LAI, chlorophyll and water contents and mesophyll structure by using the image inversion method based on an approach coupling radiative transfer modeling and a probabilistic estimation technique MCMC (Markov Chain Monte Carlo) [180].

Active microwave remote sensing imagery has also been employed, taking advantage of its ability to penetrate vegetation canopy and reach the ground surface, providing vegetation information. Molina et al. [177] assessed a methodology for characterizing vegetation canopies using optical imagery and microwave scattering models. In particular, the authors integrated biophysical variables of olive tree canopies, derived from optical images, into microwave (RADARSAT 2 imagery) scattering models.

The researches focused on phenotyping and monitoring of olive trees' biophysical parameters are summarized in the Table 4 below. In this table, a preponderance in the use of UAVs is observed.

Table 4. References dealing with phenotyping and monitoring of olive trees' biophysical parameters. The remote sensing (RS) platform used, the type of sensor and the main objectives of the researches are also indicated.

Reference	Platform	Sensor Type Used *	Aim of the Study
[178]	Satellites Sentinel-2 and PlanetScope	MS	Estimation of olive biophysical parameters
[169]	UAV DJI SPARK	RGB	Estimation of the tree row volume in super-intensive olive grove
[149]	UAV Mikrokopter	Tetracam ADC Snap (MS)	Discriminating olive cultivars with different scion/rootstock combinations
[14]	UAV - *	Tetracam MCA-6 (MS) Thermovision A40M (TH)	Estimation of parameters such LAI, chlorophyll content and water stress detection using MS and thermal UAV imagery
[164]	UAV DJI S1000	Coolpix P7700 (RGB) Tetracam ADC-lite (MS)	Estimation of biophysical and geometrical parameters of olive trees under different irrigation regimes
[115]	UAV DJI S1000	Coolpix P7700 (RGB) Tetracam ADC-lite (MS)	UAV monitoring differences in geometrical and spectral canopy characteristics between different cultivars
[148]	UAV MD4-1000	modified Sony ILCE-6000 (MS)	Development of UAV-based high-throughput system for olive breeding program applications
[145]	UAV -	modified Panasonic Lumix DMC-GF1 (MS)	Assessment of the performance of low-cost image UAV sensors for the estimation of olive crown parameters
[137]	UAV -	Sony NEX 7 (RGB)	Evaluation of UAV data in the phenotyping of canopy traits
[176]	Satellite Quickbird Aircraft -	PAN-MS CASI (HY)	Evaluating the potential of CASI and QuickBird, for mapping the tree crown size, crown transmittance and LAI *
[173]	Aircraft -	Tetracam MCA-6 (MS)	Estimation of the fraction of Intercepted Photosynthetically Active Radiation
[159]	UAV DJI Matrice 210	Sony Alpha 7 RIII (RGB) Parrot Sequoia (MS)	MS image mapping on point cloud and the multi-temporal analysis of morphological and spectral traits
[177]	Satellite RADARSAT 2	SAR	Characterizing olive grove canopies using radar data
[175]	UAV DJI Matrice 100	MicaSense RedEdge-M (MS)	Nutritional status assessment of olive crops by exploiting MS UAV imagery
[140]	UAV MD4-1000	modified Sony ILCE-6000 (MS)	UAV estimation of canopy traits for breeding program
[158]	UAV MD4-1000	Tetracam mini-MCA-6 (MS) Olympus PEN E-PM1 (RGB)	Automatic procedure for a high-throughput 3D monitoring of olive trees by using UAV imagery and OBIA *
[162]	UAV MD4-1000	Olympus PEN E-PM1 (RGB)	Optimizing acquisition UAV data procedure for DSM * generation

Table 4. *Cont.*

Reference	Platform	Sensor Type Used *	Aim of the Study
[143]	UAV MD4-1000	Sony ILCE-6000	Detecting low vigor cultivars using UAV imagery
[181]	UAV DJI Phantom 4 Pro	RGB -	Assessment of the influence of survey design and processing choices on the accuracy of tree diameter at breast height measurements
[161]	UAV -	modified Panasonic Lumix DMC-GF1 (MS)	Tree height quantification

* PAN = panchromatic; * RGB = red-green-blue; * MS = multispectral; * TH = thermal; * HY = hyperspectral; * SAR = synthetic aperture radar; * - = missing information; * LAI = leaf area index; * OBIA = object-based image analysis; * DSM = digital surface model.

6. Olive Disease Detection and Pest Management

Diseases detection is critical to preventing and limiting the loss of crop production and farm profits. Early detection of disease symptoms and their spatial extent can help contain the spread of the disease and production losses. Traditional field inspections are time-consuming, labor-intensive, and prone to human error. It can be challenging to detect the disease during the early stages when symptoms are not completely visible [182]. It is also difficult to map the spatial extent and severity of the disease spread with the traditional method of field scouting [122]. RS solves many of these problems if used to detect and monitor several diseases in different crops [183], showing itself capable of detecting diseases whose symptoms are well evident in the aerial part of the plant and those affecting the roots [184,185]. The research concerning the detection of olive disease symptoms by RS imagery has mainly focused, to our knowledge, on two diseases (Table 5): Verticillium Wilt (VW) caused by the soil-borne fungus *Verticillium Dahliae Kleb.* and Quick Decline Syndrome caused by the bacterium *Xylella fastidiosa* Wells [186] *subsp. pauca* (hereafter Xf).

Verticillium is present in the soil, in favorable conditions, in the form of resistant survival structures called 'microsclerotia' that can be stimulated to germinate by root exudates [187], generating hyphae that penetrate the roots, growing into their tissues until they reach the xylem vessels. The consequence is the spread of the fungus in the aerial parts of the plant, which causes a reduction in the water flow, inducing water stress and wilt symptoms [188–190]. In the Mediterranean area, VW's incidence and symptoms severity increase from late autumn to spring while sharply decreasing in summer, followed by a flare-up in the autumn months [191]. The most effective strategy against this disease involves using preventive control measures, in the pre- and post-planting stages [192], including irrigation management, weed control, tillage practices, soil solarization, etc. However, visual inspections to detect symptoms in the early stages are costly and time-consuming compared with the above practices, which might be more effective [191,193]. In addition, it is not conceivable to perform this strategy on each tree in olive groves of large areas [194]. The damages reported by the plant, including leaf chlorosis, defoliation, and reduced transpiration rate, can be remotely detected in the visible, Red Edge, NIR, and thermal regions of the electromagnetic spectrum [195]. In particular, the decrease of chlorophyll content in infected plants causes a higher reflectance in the visible (Green) and Red Edge, while the reduction in canopy density and leaf area corresponds to a decrease in spectral reflectance in the NIR. Furthermore, VW induces stomata closure, reducing evaporative cooling and causing an increase in leaf temperature detectable in thermal images [196]. In this regard, Calderón et al. [183] evaluated the use of thermal imagery and physiological indices derived from MS and hyperspectral sensors (mounted on UAV) for early detecting symptoms of infection caused by Verticillium in olive groves. This research showed that stomatal conductance is lower and canopy temperature variations are higher as the severity level of the disease increases. MS and hyperspectral sensors were used for calculating spectral indices related tree crown structure, epoxidation state of

the xanthophyll cycle; chlorophyll concentration and fluorescence; blue/green/red ratio indices; carotenoid concentration; spectral disease indices. Among these, the Blue band, Blue\Green ratio, Blue\Red ratio, and the fluorescence index (FLD3) were shown to be the best indicators for detecting VW, along with crown temperature and the Crop Water Stress Index (CWSI) [197] index, derived from thermal images. These indices were used by Calderón et al. [198] to formulate an automatic procedure to classify VW and its severity. Interesting in this regard is also the implementation by Blekos et al. [199] of a platform ("My Olive Grove Coach") that uses MS UAV imagery to develop an olive grove health monitoring system based on autonomous and automatic image processing using computer vision and machine learning.

Iatrou et al. [200] used NDVI and the Carotenoid Reflectance Index 2 (CRI2) [201] for detecting the early stages of VW by evaluating the spectral response of olive trees treated with Plant Growth Enhancer Formulation (PGEF). The images acquired by the UAV were compared with WorldView-2 images. Results showed that CRI2 better performed for detecting VW early stages. NDVI was shown to be better for monitoring advanced disease stages and highlighting the differences in tree spectral response due to improvements in health status following PGEF treatment. Navrozidis et al. [202] performed more recent research, which proposed a model for detecting from Sentinel-2 images stress conditions in olive groves caused by abiotic or biotic factors, including Verticillium and Xf, by exploiting the CRI2 index. Xf is a highly polyphagous plant pathogenic bacteria, infecting more than 600 species, including olive trees and stone fruits, living in a water-conducting (xylematic) system [203]. Diffusion into the xylem system, where Xf clogs the vessels, and the incubation, which can occur from 6 to 18 months, make it difficult in some cases, to identify it in the early stages [204]. Symptoms can become apparent within a few months with discoloration and wilt of the organs whose vessels have been obstructed: leaf chlorosis, crown defoliation, twig and branch die-back on the upper part of the tree crown. This symptomatic framework is ascribable to the "Olive quick decline syndrome" (OQDS) causing plant death within a few years [205–207]. Detection of the disease outbreaks, mapping its spread, and monitoring its different stages and damages to the crops is crucial for designing surveillance strategies [207,208]. The recent Xf outbreak in Europe was detected in some olive groves of the Apulia region (south-eastern Italy) (EPPO Global Database), where it rapidly spreads, carried by its vector *Philaenus spumarius* L., (*Hemiptera: Aphrophoridae*) a xylem sap-feeding insect [209]. The spread of the disease has had and is critically impacting the affected region economically and culturally-landscape-wise [210]. The defense strategy initially consisted of containment through the creation of buffer zones and eradicating infected plants (and not), especially in the case of very susceptible cultivars. In this regard, among the cultivars widespread in the Apulian territory, *Ogliarola* and *Cellina di Nardò* were highly sensitive as opposed to the cv. *Leccino* [211–213]. Studies on resistant cultivars and strategies to contain the spread of the vector insect are still ongoing. Because no effective treatment is available to eradicate Xf, and because chemical and biological control measures can only temporarily reduce the severity of the disease, prevention and containment strategies are best suited to minimize the impact of Xf [214–216]. The monitoring of Xf is based on field visual inspections. The severity of disease on olive plants can be quantified in various ways (presence or absence, intensity, level of severity) and at different scales (leaves, portions, or entire plants) [9]. Considering that the visual assessment of symptoms can be subjective in its accuracy, as well as an expensive and time-consuming practice, the role of RS is valuable here.

Similarly with VW, in the field of RS, an important aspect of identifying Xf infected plants concerns changes in the spectral reflectance of olives' canopies [217–219]. The vegetation of infected plants, characterized by less dense canopies and reduced leaf area, shows higher reflectance in the visible region, a shift in the Red Edge, and lower reflectance in the NIR [183]. The research done so far on this topic using RS platforms has concerned, to our knowledge, the monitoring of the spread of the infection and the identification, mainly in the early stages, of diseased plants. Nisio et al. [204] monitored the spreading of Xf in

Apulia by using MS UAV imagery exploiting Felsenszwalb' segmentation algorithm [220]. This algorithm foresees an over-segmentation performed on the NIR band to identify the edges of the canopies and distinguish them from the background. Two different classification methods were applied, and their results were combined. Finally, olive trees were classified into two classes according to their health status using linear discriminant analysis (LDA). Trees' health status was evaluated by using RGB, CIR, and NDVI images. Different data derived from two different platforms were used by Hornero et al. [218,221] that proposed multi-temporal data analysis, which tested the capability of VIs obtained from hyperspectral airborne campaigns and Sentinel-2 imagery to monitor the incidence and severity of Xf in olive groves. Among the VIs tested, the Atmospherically Resistant Vegetation Index (ARVI) [222] and OSAVI showed the best performances.

Other authors combined different sensors [217], data, and remote and proximal sensing data [219,223]. Poblete et al. [217] used aerial hyperspectral and thermal imagery to detect Xf infection symptoms. RS imagery was used to assess the performance of machine-learning algorithms in detecting disease symptoms. The algorithms were used to select the bands more sensitive to Xf symptoms. Authors demonstrated that disease monitoring could be performed using MS and thermal images, exploiting only a few bands selected from those most sensitive to signs: the Blue band and the CWSI index (for thermal imagery).

Zarco-Tejada et al. [219] showed early, non-visible changes in olive trees' functional traits, caused by Xf infection traits, retrieved using airborne MS and thermal imagery. While apparent symptoms such as canopy defoliation, leaf wilting, and chlorosis can be detected using NDVI, the same is not valid for other negative changes the affected plant undergoes. The authors used airborne sub metric imagery provided by hyperspectral and thermal sensors. The proposed method, which includes 260 narrow bands and the thermal region, represents an alternative to time-consuming and expensive laboratory tests. A multilayered functional plant-trait scheme was used to extract the alterations caused by Xf from several physiology-related narrow-band hyperspectral indicators. Furthermore, among the considered traits was included one consisting of temperature-based stress indicators related to stomatal conductance and alterations in plant transpiration.

Castrignanò et al. [223] tried to assess a risk assessment method based on multivariate non-parametric geostatistics, combining remote (radiometric, obtained by using MS UAV imagery), proximal (geophysical) sensor data with visual inspection data (on the field), and laboratory plant diagnostic tests. The objective was to provide probabilistic maps of Xf infection in olive trees to support its containment. The same authors also proposed [9] an integrated approach of statistical and spatial geo statistical techniques for discriminating asymptomatic and Xylella infected plants in the early stage by using MS UAV imagery. The imagery was taken on three groves different from each other in plant characteristics, age, planting pattern, and management. The approach was based on geo statistical and discriminant analysis techniques and provided a semi-automatic classification of infected plants according to the severity of symptoms.

The entomofauna phytophagous in the Mediterranean basin that insists on the olive agro-ecosystem is complex, but thanks to the many predators and parasitoids associated with it only a few species are harmful to the population dynamics and trophic activity, including the olive fly *Bactrocera oleae*. In this context, RS pest population monitoring is of great importance, especially in precision agriculture (PA), for acquiring data that are crucial for proper decision-making and pest management [224]. In olive growing, the fly *Bactrocera oleae (Diptera: Tephritidae*) is considered the most important insect pest [225]. Arid places favor fly distribution with warm summer temperatures [92]. The female fly generally lays a single egg in each olive fruit (damaging with oviposition the olives' surface), except for the presence of few fruits as opposed to a heavy population pressure [226]. When sufficient thermal energy is reached, the eggs hatch and the larvae begin to feed on the mesocarp, causing both damage to the quality of the oil and causing the olives to drop early [227–230]. Large green olives attract adult flies more than smaller ripe fruits [92]. The deterioration of oil quality is due to the development of bacterial microflora inside

the tunnels made by the larvae [225]. Subsequently, the larvae that pupate inside the fruit or in the soil become adult flies that give rise to a new generation [226,231]. The number of generations varies based on agronomic conditions and local climate, which influence reproductive activity and mortality [225,232–234]. Of course, the availability of the fruits that "host" the eggs also influences the growth of the population [226]. The only example, to our knowledge, of monitoring by RS is given by Blum et al. [235], that used the MODIS land surface temperature (LST) for estimating olive tree canopy temperature as shown in [236], and modeling olive fly populations seasonal fluctuations over a period of 11 years. Canopy temperature is considered an important variable that regulates the rate of development of immature fly stages, the rate of reproductive maturation of the adult fly, and behavioral patterns. In this research, the tree canopy temperature estimated at the pixel resolution (1 km) was used as input for the olive fly population model. The authors have experimented whether LST can be useful for simulating population fluctuations in three geographic locations differing with different climate. The reliability of the model was tested by comparing its data with those obtained in the field from trapping data. Although Bactrocera is the main insect pest of the olive tree in the world, few studies have been done currently on predictive modeling of its population dynamics [237].

The above-described olive disease detection and pest management-related researches are listed in Table 5 below.

Table 5. References dealing with the olive disease detection and pest management. The remote sensing (RS) platform used, the type of sensor and the main objectives of the researches are also indicated.

Reference	Platform	Sensor Type Used *	Aim of the Study
[199]	UAV - *	Parrot Sequoia (MS)	Implementation of an olive grove health monitoring and assessment system
[235]	Satellite Terra (EOS AM-1)	MODIS (TH)	Modeling Bactrocera Oleae population fluctuations
[183]	UAV MX-SIGHT	MCA-6 Tetracam (MS) MIRICLE 307 (TH)	Early detection of Verticillium wilt
	UAV Viewer, ELIMCO	Micro-Hyperspec VNIR (HY) MIRICLE 307 (TH)	
[198]	Aircraft CESSNA	Micro-Hyperspec VNIR model (HY) FLIR SC655 (TH)	Early detection of Verticillium wilt
[9]	UAV DJI Mavic Pro	Parrot Sequoia (MS)	Early detection of Xylella f.
[223]	UAV DJI Mavic Pro	Parrot Sequoia (MS)	Probabilistic estimation of Xylella f.
[218,221]	Aircraft CESSNA	Micro-Hyperspec VNIR model (HY)	Monitoring of Xylella f.
	Satellite Sentinel-2	MS	
[200]	UAV eBee senseFly	Multispec 4C, airinov (MS)	Early detection of Verticillium wilt
	Satellite WorldView-2	MS	
[202]	Satellite Sentinel-2	MS	Stress detection
[204]	UAV Italdron 4HSE EVO	MicaSense RedEdge-M (MS) FLIR Vue Pro 640 (TH) Sony α7r (RGB)	Xylella f. detection
[217]	Aircraft -	Micro-Hyperspec VNIR model (HY) FLIR SC655 (TH)	Monitoring of Xylella f.
[219]	Aircraft -	Micro-Hyperspec VNIR model (HY) FLIR SC655 (TH)	Early detection of Xylella f.

* MS = multispectral; * TH = thermal; * HY = hyperspectral; * RGB = red-green-blue; * - = missing information.

7. Final Remarks and Future Challenges

To the best of our knowledge, most of the research on the applications examined in this review has concerned tree detection and counting, phenotyping and monitoring of biophysical parameters, and disease detection and management of irrigation resources (a topic covered in the review by Messina and Modica [10]). In the first decade of the 2000s, of only 12 studies identified, as shown in Figure 1, 11 concerned tree detection and counting, highlighting how the topic represented one of the first 'challenges' of RS in olive growing at that time. More research was observed concerning the use of satellites for tree detection and counting, while greater use of UAVs has been made in phenotyping research. Regarding

tree detection, this is due to research carried out [11–13,15,19,22] in the first decade of the 2000s exploiting satellite imagery with sufficient spatial resolution (from 0.6 to 2.5 m) to detect and count individual canopies, such as those from Quickbird and IKONOS [21], and before the spread of UAVs. As far as phenotyping research is concerned, the increase in the use of UAVs is probably due to their greater suitability than satellites in cloudy conditions when investigating small areas needing centimeter spatial resolution (1–2 cm depending on flying altitude) and greater temporal resolution [43,122,135,238]. UAVs can be exploited multiple times during a brief period to acquire centimetric information, while most satellites do not provide data at the centimeter scale needed for several field-scale PA applications. In research focused on olive disease detection, Sentinel-2 satellites, aircrafts, and UAVs mounting different sensors (MS, thermal, and hyperspectral) over the surveyed period have been similarly extensive. In the comparison between the subject matter most frequently addressed at the beginning of the twentieth century, exclusively using satellite images at low and medium resolutions, and more recent topics such as phenotyping and disease detection, which benefit from very high satellite and UAV spatial and temporal resolutions, the gradual technical advancement of RS in the field of agri-environmental analyses is revealed. The strengths and weaknesses of satellites and UAVs are evident when the goal is to detect disease symptoms early. UAVs are not the ideal platform for monitoring large areas, but they are generally able to provide images with a higher spatial and temporal resolution, especially in the case of thermal images, so they are useful in the monitoring of olive diseases such as Xylella and Verticillium at early stages [183]. UAVs can be used in two stages of disease control: in the early stages by detecting a possible infection before visible symptoms appear, or mapping the infection's size in different parts of a crop. In the latter case, the farmer will have a clearer map of the affected areas and support in making early decisions to reduce losses. At intermediate-advanced stages, UAVs can be used during the treatment of the infection for targeted spraying and monitoring [239]. On the other hand, as shown in [218], images from the Sentinel-2 (available with a frequency of 2–3 days) can be useful for large-scale monitoring of the spread of Xf at intermediate to severe stages. As stated by Castrignanò et al. and Barbedo [9,240], results from using different types of sensors over an area, including proximal, UAV-mounted, aircraft-mounted, and satellite-mounted indicate benefits from complementary rather than competitive use. Several authors have proposed combining images acquired with different platforms as UAVs and satellites and at different spatial scales aiming at a data fusion approach to improve stress detection capability [9,241]. In addition, combining RS data with different types of data, including weather information, historical data on disease incidence, and information on agronomic practices in the field, will allow for more efficient disease monitoring [199]. These considerations are valid not only in disease detection. Generally, the data fusion from remote and proximal sensors should be coupled with well-defined protocols by which spatial congruence between the sensors and the data provided by the laboratory's analysis is achieved. Regarding the data field collection, an important contribution can come from the Internet of Things (IoT), which allows "on-site monitoring" remotely farms [242]. IoT has increasingly developed thanks to scientists, researchers, and engineers implementing new technologies, methods to monitor crops, and facilitating access to agricultural data (such as crop-related and meteorological data) critical in the analysis and prediction of phenology and implementation of the yield forecasting models [123,128]. This momentum offers many possibilities for optimizing procedures and adapting these technologies in PA [243]. However, the current trend sees PA products primarily directed towards large area farms and agricultural companies equipped with advanced machinery and tools, with technology providers and data companies seemingly uninterested in collecting and processing small farm data [244]. Given the complexity of image processing methods and the expertise required for RS data management, it is necessary to develop a reliable yet simple workflow for real-time data analysis and extraction. For example, artificial intelligence techniques, such as machine learning, could generate spatially and temporally continuous data from satellites at a scale necessary for PA applications [245]. Facilitating

the acquisition and processing of RS data is also an important challenge in increasing the pool of users able to access and use RS technologies in agriculture [122].

Other challenges relate to data, particularly the need to standardize procedures for converting images into prescription maps, classification maps, and VIs maps, the latter was used in much of the research examined in this review, as shown in Table 6.

Table 6. The vegetation indices (VIs) used in remote sensing (RS) researches in olive growing.

Vegetation Index (VI)	Acronym	Equation	Research
Chlorophyll Vegetation Index [246]	CVI	$NIR \frac{Red}{(Green)^2}$	[43]
Difference Vegetation Index [155]	DVI	NIR-Red	[149]
Enhanced Vegetation Index [247]	EVI	$G \frac{(NIR-Red)}{(NIR+CRed-CBlue+L)}$	[128,198]
Enhanced Vegetation Index 2 [248]	EVI 2	$\frac{2.5(NIR-Red)}{(NIR+2.4Red+L)}$	[149]
Generalized difference Vegetation Index [249]	GDVI	$\frac{SR^n-1}{SR^n+1}$**	[149]
Green Ratio Vegetation Index [171]	GRVI	$\frac{NIR}{Green}$	[115,159,198]
Normalized Difference Red Edge Index [250]	NDRE	$\frac{(NIR-Red\ Edge)}{(NIR+Red\ Edge)}$	[43,49,159]
Green and Red Normalized Difference Vegetation Index [152]	GRNDVI	$\frac{NIR-(Green+Red)}{NIR+(Green+Red)}$	[43,115,149]
Green Normalized Vegetation Index [151]	GNDVI	$\frac{(NIR-Green)}{(NIR+Green)}$	[42,43,115,149,218]
Modified chlorophyll absorption in reflectance index [56]	$MCARI_2$	$\frac{1.5(2.5(NIR-Red)-1.3(NIR-Green))}{\sqrt{(2NIR+1)^2-(6NIR-5\sqrt{Red})-0.5}}$	[49]
Modified Simple Ratio [251]	MSR	$\frac{(NIR/Red-1)}{\sqrt{NIR/Red+1}}$	[176,183,198,218]
Modified Soil Adjusted Vegetation Index [54]	MSAVI	$[2\ NIR + 1 - [(2\ NIR + 1)^2 - 8(NIR - Red)]^{1/2}]/2$	[49,115,149,218]
Modified triangular vegetation index [56]	$MTVI_1$	$1.2 \times [1.2(NIR - Green) - 2.5(Red - Green)]$	[149,183,198]
Normalized difference green/red index [154]	NGRDI	$\frac{(Green-Red)}{(Green+Red)}$	[149]
Normalized Difference Vegetation Index [46]	NDVI	$\frac{(NIR-Red)}{(NIR+Red)}$	[20,21,43,48,49,78,82,115,120,123,128,131,149,159,164,173,176,183,198,200,202,204,218,219,221,235,252,253]
Optimized Soil Adjusted Vegetation Index [167]	OSAVI	$1.16 \frac{(NIR-Red)}{(NIR+Red+0.16)}$	[149,183,198,218,221,253]
Photochemical Reflectance Index (570) [165]	PRI 570	$(R_{570} - R_{531})/(R_{570} + R_{531})$ *	[183,198]
Perpendicular Vegetation Index [155]	PVI	$\sqrt{\left(Red^{Veg} - Red^{Soil}\right)^2 + \left(NIR^{Veg} - NIR^{Soil}\right)^2}$	[218]
Ratio Vegetation Index [155]	IRVI	$\frac{Red}{NIR}$	[149]

Table 6. *Cont.*

Vegetation Index (VI)	Acronym	Equation	Research
Renormalized Difference Vegetation Index [254]	RDVI	$\frac{(NIR-Red)}{\sqrt{(NIR+Red)}}$	[78,176,183,198]
Simple Ratio [150]	SR	$\frac{NIR}{Red}$	[20,149,159,176,183,218]
Soil Adjuted Vegetation Index [255]	SAVI	$\frac{(NIR-Red)}{(NIR+Red+L)}(1+L)$ ***	[43]
Transformed Chlorophyll Absorption in Reflectance Index [166]	TCARI	$3[(NIR\text{-}Red) - 0.2(NIR - Green)(NIR/Red)]$	[183,198,218]
Transformed Chlorophyll Absorption in Reflectance Index/Optimized Soil-Adjusted Vegetation Index [166]	TCARI/OSAVI	$\frac{3[(NIR-Red)-0.2(NIR-Green)(NIR/Red)]}{((1+0.16)(NIR-Red)/(NIR+Red+0.16)}$	[198,218,253]
Transformed Vegetation Index [55]	TVI	$(NDVI + 0.5)^{0.5}$	[149]
Triangular Vegetation Index [55]	TVI	$\frac{1}{2}$ [120 (NIR − Green) − 200 (NIR − Green)]	[183,198]
Vogelmann Red Edge Index [256]	VREI	$\frac{NIR}{Red\ Edge}$	[183,198]

* R = reflectance; ** = n is an integer > 0; *** L = soil adjustment factor ranging from 0 to 1.

This leads to using different research methods to achieve the same goal with results that are not always excellent or reliable [239]. The presence of different software for image analysis with different complexity in usage, capacities, and prices constitutes a further uncertainty in the choices of the company or farmer. In this regard, some images can be provided to the farmer pre processed and in a "form" that is already usable according to their needs. On the other hand, it is difficult to easily find reliable data, such as time-series images, in the absence of standard procedures for aspects such as radiometric calibration and retrieval of reflectance and temperature data [257]. Despite a large number of studies on RS applications in PA, there is a general lack of established techniques and/or frameworks that are accurate, reproducible, and applicable under a wide variety of climatic, soil, crop, and management conditions. The accuracy of methods using RS platforms data (satellite, airborne, and UAV) depends on a variety of factors, including image resolution (spatial, spectral, and temporal); atmospheric, climatic, and weather conditions; crop and field conditions (e.g., growth stage, land cover); and the analyses technique (e.g., regression-based, machine learning, physically-based modeling). In this regard, a big push in automating remote enterprise data analysis can come from increased interoperability between field sensors that collect real-time data, and proximal and remote sensing sensors. The considerations made so far on RS platforms, such as the need for the standardization of methods of data collection, processing and output production, dissemination and transmission of knowledge, and expertise from the scientific field to companies in the sector and farms, are valid both for the olive sector as for other crops. The resolution of these issues is a necessary step for the modernization of the sector. The olive sector is very complex because, unlike other agricultural realities, it is spread over several continents and different parts of the world with different climatic and environmental conditions that alone are sufficient to generate different needs from the agronomic and technological point of view. These needs focus interest, including research, on different issues. Even the management of an olive farm is heterogeneous from country to country. Just think of Italian olive-growing, characterized by the coexistence of traditional and intensive systems, or as in Spain with a super-intensive system spread mainly in the Andalusia region [258–260]. First of all, it must be considered that the size of a company inevitably determines the availability of the

economy, and its interest in investing in expensive technologies that do not always lead to increases in production and revenue to justify technological modernization. Other times the limits are not dictated only by the size but by the location of olive-grown areas, seen in the phenomenon of excessive fragmentation (present in some Italian realities with many farms with average surface of less than 2 ha) [260], the prevalence of traditional olive groves in marginal areas, and difficult to mechanize whose persistent presence is justified both by the conformation of the territory (Greece and Italy) and by the agricultural policies of these countries. Often the decision to maintain traditional planting systems at the expense of the rejuvenation of olive groves and modernization depends on the desire to preserve local cultivars. An example is Italian olive growing, whose biodiversity, with over 630 cultivars, represents 40% of the world heritage [260–262]. In this framework, olive planting systems resulted in obsolete production structures with high costs and low profits due to poor mechanization [260]. This has repercussions on practical aspects of agronomic management, such as pruning and harvesting, which are among the most onerous operations that can be fully mechanized or not according with the characteristics of the olive grove and the availability of farm funds [27,263,264]. The survival of this sector is linked to the possibility of fully mechanizing harvest and as much as possible pruning [265,266]. This, in turn, determines the interface between olive growers and research, the issues also addressed in the field of research in RS. Among other things, steps forward in research in a field are not always immediate. Still, some of them result from developments and discoveries in other areas or effective experimentation on other crops, perhaps more fashionable, discussed, and profitable. In any case, comparing what has been done and what is currently being done on other crops, we do not see the olive tree lagging behind concerning the implementation of strategies involving the use of RS, but perhaps in the use of RS. This, as already said, is not so much due to research as much as the need for a new organization of the sector. This goal can be achieved through combining different scientific, technical, and entrepreneurial skills and adjusting farming management strategies with best practices, policies, and financial instruments. Larger mechanization is a priority objective, and proper management of water resources given the present and future consequences of climate change [267]. In particular, the southern Mediterranean is expected to be the most affected by climate change, with reduced yields and degraded ecosystems due to rising temperatures, increased drought risk, and decreased water availability [3]. The current trend dictated by PA requires more precision, data sharing, the ready availability of data and communication, not only between machines but also between all the actors involved in the production line bringing benefits from production, quality, and environmental perspectives [1,27]. Consumers are gaining more awareness of the influence of food on human health, thus promoting products with preventive and therapeutic properties [92,268]. Extra virgin olive oil and table olives may be considered nutraceutical products rich in antioxidant compounds and have cardiovascular health benefits [269,270]. This drives more financially sound markets, including Japan, USA, China, and the United Arab Emirates, to demand and pay more for healthy products, especially if they are produced in "green" ways, i.e., low environmental impact production techniques [27]. To be rewarded in this sense is also the use of local biodiversity, which also increases the health and functional value of foods and their sensory attributes. For this reason, the sole objective of the sector the modernization of the company should not be aimed exclusively at high production focusing on cultivars suitable for mechanization and super-intensive plantings. The quality of a product such as olive oil also passes through the enhancement of autochthonous and minor cultivars, while promoting the economic development of specific territories and preserving biodiversity. As seen from the research done so far, RS can make an important contribution in solving the main challenges that olive growing will face.

The latest discoveries in nutrition that see a product, in particular, extra virgin olive oil, as a harbinger of many benefits in terms of health produced a renewed interest, which is a favorable point that can encourage research and technological development to invest and apply more towards olive growing, which although practiced since ancient times,

represents both the traditions and the future of many agricultural realities in Mediterranean countries and beyond.

Author Contributions: Conceptualization, methodology, investigation, data curation, writing—review and editing, G.M. (Gaetano Messina) and G.M. (Giuseppe Modica). All authors have read and agreed to the published version of the manuscript.

Funding: This research received no external funding.

Conflicts of Interest: The authors declare no conflict of interest.

References

1. Roma, E.; Catania, P. Precision Oliviculture: Research Topics, Challenges, and Opportunities—A Review. *Remote Sens.* **2022**, *14*, 1668. [CrossRef]
2. Anastasiou, E.; Balafoutis, A.T.; Fountas, S. Trends in Remote Sensing Technologies in Olive Cultivation. *Smart Agric. Technol.* **2023**, *3*, 100103. [CrossRef]
3. Michalopoulos, G.; Kasapi, K.A.; Koubouris, G.; Psarras, G.; Arampatzis, G.; Hatzigiannakis, E.; Kavvadias, V.; Xiloyannis, C.; Montanaro, G.; Malliaraki, S.; et al. Adaptation of Mediterranean olive groves to climate change through sustainable cultivation practices. *Climate* **2020**, *8*, 54. [CrossRef]
4. Sarabia, R.; Aquino, A.; Ponce, J.M.; López, G.; Andújar, J.M. Automated identification of crop tree crowns from uav multispectral imagery by means of morphological image analysis. *Remote Sens.* **2020**, *12*, 748. [CrossRef]
5. Nolè, G.; Pilogallo, A.; Lanortea, A.; De Santisa, F. Remote Sensing Techniques in Olive-Growing: A Review. *Curr. Investig. Agric. Curr. Res.* **2018**, *2*, 205–208. [CrossRef]
6. Rosati, A.; Paoletti, A.; Caporali, S.; Perri, E. The role of tree architecture in super high density olive orchards. *Sci. Hortic.* **2013**, *161*, 24–29. [CrossRef]
7. Fabbri, A.; Lambardi, M. Ozden-Tokatli Olive Breeding. In *Breeding Plantation Tree Crops: Tropical Species*; Mohan Jain, S., Priyardashan, P.M., Eds.; Springer: New York, NY, USA, 2009; pp. 423–465.
8. Saponari, M.; Giampetruzzi, A.; Loconsole, G.; Boscia, D.; Saldarelli, P. Xylella fastidiosa in Olive in Apulia: Where We Stand. *Phytopathology* **2019**, *109*, 175–186. [CrossRef] [PubMed]
9. Castrignanò, A.; Belmonte, A.; Antelmi, I.; Quarto, R.; Quarto, F.; Shaddad, S.; Sion, V.; Muolo, M.R.; Ranieri, N.A.; Gadaleta, G.; et al. Semi-automatic method for early detection of xylella fastidiosa in olive trees using uav multispectral imagery and geostatistical-discriminant analysis. *Remote Sens.* **2021**, *13*, 14. [CrossRef]
10. Messina, G.; Modica, G. Twenty years of remote sensing applications targeting landscape analysis and environmental issues in olive growing: A review. *Remote Sens.* **2022**, *14*, 5430. [CrossRef]
11. Barata, T.; Pina, P. Morphological Recognition of Olive Grove Patterns. In *Iberian Conference on Pattern Recognition and Image Analysis*; Springer: Berlin/Heidelberg, Germany, 2003; pp. 89–96. ISBN 0302-9743.
12. Masson, J.; Soille, P.; Mueller, R. Tests with VHR images for the identification of olive trees and other fruit trees in the European Union. *Proc. Remote Sens. Agric. Ecosyst. Hydrol. VI* **2004**, *5568*, 23–36. [CrossRef]
13. Nihal, C.; Ediz, U.; Masson, J. A Case Study of Developing An Olive Tree Database for Turkey. *Photogramm. Eng. Remote Sens.* **2009**, *75*, 1397–1405.
14. Berni, J.; Zarco-Tejada, P.J.; Suarez, L.; Fereres, E. Thermal and Narrowband Multispectral Remote Sensing for Vegetation Monitoring From an Unmanned Aerial Vehicle. *IEEE Trans. Geosci. Remote Sens.* **2009**, *47*, 722–738. [CrossRef]
15. Karantzalos, K.G.; Argialas, D.P. Towards automatic olive tree extraction from satellite imagery. In Proceedings of the Geo-Imagery Bridging Continents. XXth ISPRS Congress, Istanbul, Turkey, 12–23 July 2004; pp. 12–23.
16. Kallel, A.; Masmoudi, D.S.; Salhi, M.; Amine, M.; Aïcha, B.; Khanfir, I. A new Wavelet based Multi-Resolution Texture Segmentation scheme of Remotely Sensed Images for Vegetation Extraction. In Proceedings of the 1st International Conference on Signal-Image Technology and Internet-Based Systems, SITIS 2005, Yaounde, Cameroon, 27 November–1 December 2005; pp. 70–76.
17. Robbez-Masson, J.M.; Foltête, J.C. Localising missing plants in squared-grid patterns of discontinuous crops from remotely sensed imagery. *Comput. Geosci.* **2005**, *31*, 900–912. [CrossRef]
18. Karantzalos, K.; Argialas, D. Improving edge detection and watershed segmentation with anisotropic diffusion and morphological levellings. *Int. J. Remote Sens.* **2006**, *27*, 5427–5434. [CrossRef]
19. Gonzalez, J.; Galindo, C.; Arevalo, V.; Ambrosio, G. Applying image analysis and probabilistic techniques for counting olive trees in high-resolution satellite images. In *Advanced Concepts for Intelligent Vision Systems*; Lecture Notes in Computer Science; Springer: Berlin/Heidelberg, Germany, 2007; Volume 4678, pp. 920–931. [CrossRef]
20. García Torres, L.; Peña-Barragán, J.M.; López-Granados, F.; Jurado-Expósito, M.; Fernández-Escobar, R. Automatic assessment of agro-environmental indicators from remotely sensed images of tree orchards and its evaluation using olive plantations. *Comput. Electron. Agric.* **2008**, *61*, 179–191. [CrossRef]
21. Daliakopoulos, I.N.; Grillakis, E.G.; Koutroulis, A.G.; Tsanis, L.K. Tree crown detection on multispectral VHR satellite imagery. *Photogramm. Eng. Remote Sens.* **2009**, *75*, 1201–1211. [CrossRef]

22. Bazi, Y.; Al-Sharari, H.; Melgani, F. An automatic method for counting olive trees in very high spatial remote sensing images. In Proceedings of the 2009 IEEE International Geoscience and Remote Sensing Symposium, Cape Town, South Africa, 12–17 July 2009; pp. II-125–II-128. [CrossRef]
23. Hung, C.; Bryson, M.; Sukkarieh, S. Multi-class predictive template for tree crown detection. *ISPRS J. Photogramm. Remote Sens.* **2012**, *68*, 170–183. [CrossRef]
24. Ye, Z.; Wei, J.; Lin, Y.; Guo, Q.; Zhang, J.; Zhang, H.; Deng, H.; Yang, K. Extraction of Olive Crown Based on UAV Visible Images and the U2-Net Deep Learning Model. *Remote Sens.* **2022**, *14*, 1523. [CrossRef]
25. Waleed, M.; Um, T.W.; Khan, A.; Khan, U. Automatic detection system of olive trees using improved K-means algorithm. *Remote Sens.* **2020**, *12*, 760. [CrossRef]
26. Pina, P.; Barata, T.; Bandeira, L. Morphological recognition of the spatial patterns of olive trees. *Proc.-Int. Conf. Pattern Recognit.* **2006**, *4*, 845–848. [CrossRef]
27. Lo Bianco, R.; Proietti, P.; Regni, L.; Caruso, T. Planting Systems for Modern Olive Growing: Strengths and Weaknesses. *Agriculture* **2021**, *11*, 494. [CrossRef]
28. Osco, L.P.; Marcato Junior, J.; Marques Ramos, A.P.; de Castro Jorge, L.A.; Fatholahi, S.N.; de Andrade Silva, J.; Matsubara, E.T.; Pistori, H.; Gonçalves, W.N.; Li, J. A review on deep learning in UAV remote sensing. *Int. J. Appl. Earth Obs. Geoinf.* **2021**, *102*, 102456. [CrossRef]
29. Khan, A.; Khan, U.; Waleed, M.; Khan, A.; Kamal, T.; Marwat, S.N.K.; Maqsood, M.; Aadil, F. Remote Sensing: An Automated Methodology for Olive Tree Detection and Counting in Satellite Images. *IEEE Access* **2018**, *6*, 77816–77828. [CrossRef]
30. Waleed, M.; Um, T.W.; Khan, A.; Ahmad, Z. An Automated Method for Detection and Enumeration of Olive Trees through Remote Sensing. *IEEE Access* **2020**, *8*, 108592–108601. [CrossRef]
31. Salamí, E.; Gallardo, A.; Skorobogatov, G.; Barrado, C. On-the-fly olive tree counting using a UAS and cloud services. *Remote Sens.* **2019**, *11*, 316. [CrossRef]
32. Osco, L.; Mauro dos Santos de Marcato Junior, J.A.; da Silva, N.B.; Ramos, A.P.M.; Moryia, É.A.S.; Imai, N.N.; Pereira, D.R.; Creste, J.E.; Matsubara, E.T.; Li, J.; et al. A convolutional neural network approach for counting and geolocating citrus-trees in UAV multispectral imagery. *ISPRS J. Photogramm. Remote Sens.* **2020**, *160*, 97–106. [CrossRef]
33. Meyer, F. Cytologie Quantitative et Morphologie Mathématique. Ph.D. Thesis, École Nationale Supérieure des Mines de Paris, Paris, France, 1979.
34. Otsu, N. A Threshold Selection Method from Gray-Level Histograms. *IEEE Trans. Syst. Man. Cybern.* **1979**, *9*, 62–66. [CrossRef]
35. Duda, R.O.; Hart, P.E. Use of the Hough Transformation to Detect Lines and Curves in Pictures. *Commun. ACM* **1972**, *15*, 11–15. [CrossRef]
36. Rasmussen, C.E. Gaussian Process for Machine Learning. In *Advanced Lectures on Machine Learning*; Springer: Berlin/Heidelberg, Germany, 2017; pp. 6926–6935.
37. Soille, P. *Morphological Image Analysis: Principles and Applications*; Springer: Berlin/Heidelberg, Germany, 2004; ISBN 978-3-642-08445-4. [CrossRef]
38. Canny, J. A Computational Approach to Edge Detection. *IEEE Trans. Pattern Anal. Mach. Intell.* **1986**, *PAMI-8*, 679–698. [CrossRef]
39. Akmal Butt, M.; Maragos, P. Optimum design of chamfer distance transforms. *IEEE Trans. Image Process.* **1998**, *7*, 1477–1484. [CrossRef]
40. Ozen, F.; Bolca, M. The Compare of OliveTree Counting Methods. *Fresenius Environ. Bull.* **2020**, *29*, 1655–1667.
41. De Castro, A.I.; Torres-Sánchez, J.; Peña, J.M.; Jiménez-Brenes, F.M.; Csillik, O.; López-Granados, F. An automatic random forest-OBIA algorithm for early weed mapping between and within crop rows using UAV imagery. *Remote Sens.* **2018**, *10*, 285. [CrossRef]
42. Modica, G.; De Luca, G.; Messina, G.; Praticò, S. Comparison and assessment of different object-based classifications using machine learning algorithms and UAVs multispectral imagery: A case study in a citrus orchard and an onion crop. *Eur. J. Remote Sens.* **2021**, *54*, 431–460. [CrossRef]
43. Modica, G.; Messina, G.; De Luca, G.; Fiozzo, V.; Praticò, S. Monitoring the vegetation vigor in heterogeneous citrus and olive orchards. A multiscale object-based approach to extract trees' crowns from UAV multispectral imagery. *Comput. Electron. Agric.* **2020**, *175*, 105500. [CrossRef]
44. Zisi, T.; Alexandridis, T.K.; Kaplanis, S.; Navrozidis, I.; Tamouridou, A.A.; Lagopodi, A.; Moshou, D.; Polychronos, V. Incorporating surface elevation information in UAV multispectral images for mapping weed patches. *J. Imaging* **2018**, *4*, 132. [CrossRef]
45. Jones, H.G.; Vaughan, R.A. *Remote Sensing of Vegetation Principles, Techniques, and Applications*; Oxford University Press: Oxford, UK, 2010; ISBN 9780199207794.
46. Rouse, W.; Haas, R.H.; Deering, D.W. *Monitoring Vegetation Systems in the Great Plains with ERTS*; Goddard Space Flight Center 3d ERTS-1 Symp; NASA: Washington, DC, USA, 1974; Volume 1.
47. Birth, G.S.; McVey, G.R. Measuring the Color of Growing Turf with a Reflectance Spectrophotometer 1. *Agron. J.* **1968**, *60*, 640–643. [CrossRef]
48. Karydas, C.; Gewehr, S.; Iatrou, M.; Iatrou, G.; Mourelatos, S. Olive Plantation Mapping on a Sub-Tree Scale with Object-Based Image Analysis of Multispectral UAV Data; Operational Potential in Tree Stress Monitoring. *J. Imaging* **2017**, *3*, 57. [CrossRef]

49. Solano, F.; Di Fazio, S.; Modica, G. A methodology based on GEOBIA and WorldView-3 imagery to derive vegetation indices at tree crown detail in olive orchards. *Int. J. Appl. Earth Obs. Geoinf.* **2019**, *83*, 101912. [CrossRef]
50. Baatz, M.; Schäpe, A. Multi-resolution segmentation: An optimization approach for high quality multi-scale. In Proceedings of the Beiträge zum, Agit XII Symposium Salsburg, Heidelberg, Germany; 2000; pp. 12–23. [CrossRef]
51. Hay, G.J.; Castilla, G. Object-based image analysis: Strengths, weaknesses, opportunities and threats (SWOT). In *Proceedings of the International Archives of the Photogrammetry*; Remote Sensing and Spatial Information Sciences: Hannover, Germany, 2006; pp. 4–5. Available online: http://www.isprs.org/proceedings/XXXVI/4-C42/Papers/01_OpeningSession/OBIA2006_Hay_Castilla.pdf (accessed on 1 September 2022).
52. Cheng, G.; Han, J. A survey on object detection in optical remote sensing images. *ISPRS J. Photogramm. Remote Sens.* **2016**, *117*, 11–28. [CrossRef]
53. Barnes, E.M.; Clarke, T.R.; Richards, S.E.; Colaizzi, P.D.; Haberland, J.; Kostrzewski, M.; Waller, P.; Choi, C.; Riley, E.; Thompson, T.; et al. Coincident detection of crop water stress, nitrogen status and canopy density using ground based multispectral data. In Proceedings of the Fifth International Conference on Precision Agriculture, Bloomington, MN, USA, 16–19 July 2000.
54. Qi, J.; Chehbouni, A.; Huete, A.R.; Kerr, Y.H.; Sorooshian, S. A modified soil adjusted vegetation index. *Remote Sens. Environ.* **1994**, *48*, 119–126. [CrossRef]
55. Broge, N.; Leblanc, E. Comparing prediction power and stability of broadband and hyperspectral vegetation indices for estimation of green leaf area index and canopy chlorophyll density. *Remote Sens. Environ.* **2001**, *76*, 156–172. [CrossRef]
56. Haboudane, D.; Miller, J.R.; Pattey, E.; Zarco-Tejada, P.J.; Strachan, I.B. Hyperspectral vegetation indices and novel algorithms for predicting green LAI of crop canopies: Modeling and validation in the context of precision agriculture. *Remote Sens. Environ.* **2004**, *90*, 337–352. [CrossRef]
57. Eckert, S. Improved Forest Biomass and Carbon Estimations Using Texture Measures from WorldView-2 Satellite Data. *Remote Sens.* **2012**, *4*, 810–829. [CrossRef]
58. Pu, R.; Landry, S. A comparative analysis of high spatial resolution IKONOS and WorldView-2 imagery for mapping urban tree species. *Remote Sens. Environ.* **2012**, *124*, 516–533. [CrossRef]
59. Wolf, A.F. Using WorldView-2 Vis-NIR multispectral imagery to support land mapping and feature extraction using normalized difference index ratios. In Proceedings of the Algorithms and Technologies for Multispectral, Hyperspectral, and Ultraspectral Imagery XVIII, Baltimore, MD, USA, 23–27 April 2012; Shen, S.S., Lewis, P.E., Eds.; pp. 188–195.
60. Crabbe, R.A.; Lamb, D.; Edwards, C. Discrimination of species composition types of a grazed pasture landscape using Sentinel-1 and Sentinel-2 data. *Int J Appl Earth Obs Geoinf.* **2020**, *84*, 101978. [CrossRef]
61. Peña, J.M.; Gutiérrez, P.A.; Hervás-Martínez, C.; Six, J.; Plant, R.E.; López-Granados, F. Object-based image classification of summer crops with machine learning methods. *Remote Sens.* **2014**, *6*, 5019–5041. [CrossRef]
62. Perez-Ortiz, M.; Gutierrez, P.A.; Pena, J.M.; Torres-Sanchez, J.; Lopez-Granados, F.; Hervas-Martinez, C. Machine learning paradigms for weed mapping via unmanned aerial vehicles. In Proceedings of the 2016 IEEE Symposium Series on Computational Intelligence (SSCI), Athens, Greece, 6–9 December 2016. [CrossRef]
63. Abdulridha, J.; Batuman, O.; Ampatzidis, Y. UAV-Based Remote Sensing Technique to Detect Citrus Canker Disease Utilizing Hyperspectral Imaging and Machine Learning. *Remote Sens.* **2019**, *11*, 1373. [CrossRef]
64. Cao, F.; Liu, F.; Guo, H.; Kong, W.; Zhang, C.; He, Y. Fast detection of sclerotinia sclerotiorum on oilseed rape leaves using low-altitude remote sensing technology. *Sensors* **2018**, *18*, 4464. [CrossRef]
65. De Luca, G.; Silva, J.M.N.; Cerasoli, S.; Araújo, J.; Campos, J.; Di Fazio, S.; Modica, G. Object-Based Land Cover Classification of Cork Oak Woodlands using UAV Imagery and Orfeo ToolBox. *Remote Sens.* **2019**, *11*, 1238. [CrossRef]
66. Praticò, S.; Solano, F.; Di Fazio, S.; Modica, G. Machine Learning Classification of Mediterranean Forest Habitats in Google Earth Engine Based on Seasonal Sentinel-2 Time-Series and Input Image Composition Optimisation. *Remote Sens.* **2021**, *13*, 586. [CrossRef]
67. Qian, Y.; Zhou, W.; Yan, J.; Li, W.; Han, L. Comparing machine learning classifiers for object-based land cover classification using very high resolution imagery. *Remote Sens.* **2015**, *7*, 153–168. [CrossRef]
68. Noi, P.T.; Kappas, M. Comparison of random forest, k-nearest neighbor, and support vector machine classifiers for land cover classification using sentinel-2 imagery. *Sensors* **2018**, *18*, 18. [CrossRef]
69. De Luca, G.; Silva, J.M.N.; Di Fazio, S.; Modica, G. Integrated use of Sentinel-1 and Sentinel-2 data and open-source machine learning algorithms for land cover mapping in a Mediterranean region. *Eur. J. Remote Sens.* **2022**, *55*, 52–70. [CrossRef]
70. Rehman, T.U.; Mahmud, M.S.; Chang, Y.K.; Jin, J.; Shin, J. Current and future applications of statistical machine learning algorithms for agricultural machine vision systems. *Comput. Electron. Agric.* **2019**, *156*, 585–605. [CrossRef]
71. Liakos, K.G.; Busato, P.; Moshou, D.; Pearson, S.; Bochtis, D. Machine learning in agriculture: A review. *Sensors* **2018**, *18*, 2674. [CrossRef] [PubMed]
72. Cortes, C.; Vapnik, V. Support-Vector Networks Editor. *Mach. Learn.* **1995**, *20*, 273–297. [CrossRef]
73. Vapnik, V. *Statistical Learning Theory*; Wiley and Sons: New York, NY, USA, 1998; ISBN 978-0-471-03003-4.
74. Breiman, L. Random forests. *Mach. Learn.* **2001**, *45*, 5–32. [CrossRef]
75. Grizonnet, M.; Michel, J.; Poughon, V.; Inglada, J.; Savinaud, M.; Cresson, R. Orfeo ToolBox: Open source processing of remote sensing images. *Open Geospat. Data Softw. Stand.* **2017**, *2*, 15. [CrossRef]

76. Pedregosa, F.; Varoquaux, G.; Gramfort, A.; Michel, V.; Thirion, B.; Grisel, O.; Blondel, M.; Prettenhofer, P.; Weiss, R.; Dubourg, V.; et al. Scikit-learn: Machine learning in Python. *J. Mach. Learn. Res.* **2011**, *12*, 2825–2830.
77. Varoquaux, G.; Buitinck, L.; Louppe, G.; Grisel, O.; Pedregosa, F.; Mueller, A. Scikit-learn. *GetMobile Mob. Comput. Commun.* **2015**, *19*, 29–33. [CrossRef]
78. Castillejo-González, I.L. Mapping of olive trees using pansharpened Quickbird images: An evaluation of pixel- and object-based analyses. *Agronomy* **2018**, *8*, 288. [CrossRef]
79. Lu, D.; Weng, Q. A survey of image classification methods and techniques for improving classification performance. *Int. J. Remote Sens.* **2007**, *28*, 823–870. [CrossRef]
80. Šiljeg, A.; Panđa, L.; Domazetović, F.; Marić, I.; Gašparović, M.; Borisov, M.; Milošević, R. Comparative Assessment of Pixel and Object-Based Approaches for Mapping of Olive Tree Crowns Based on UAV Multispectral Imagery. *Remote Sens.* **2022**, *14*, 757. [CrossRef]
81. Peters, J.; Van Coillie, F.; Westra, T.; De Wulf, R. Synergy of very high resolution optical and radar data for object-based olive grove mapping. *Int. J. Geogr. Inf. Sci.* **2011**, *25*, 971–989. [CrossRef]
82. Akcay, H.; Kaya, S.; Sertel, E.; Alganci, U. Determination of olive trees with multi-sensor data fusion. In Proceedings of the 8th International Conference on Agro-Geoinformatics, Agro-Geoinformatics 2019, Istanbul, Turkey, 16–19 July 2019; pp. 1–6. [CrossRef]
83. ESA Copernicus Open Access Hub. Available online: https://scihub.copernicus.eu/ (accessed on 12 February 2022).
84. Huang, H.; Lan, Y.; Yang, A.; Zhang, Y.; Wen, S.; Deng, J. Deep learning versus Object-based Image Analysis (OBIA) in weed mapping of UAV imagery. *Int. J. Remote Sens.* **2020**, *41*, 3446–3479. [CrossRef]
85. Zhong, L.; Hu, L.; Zhou, H. Deep learning based multi-temporal crop classification. *Remote Sens. Environ.* **2019**, *221*, 430–443. [CrossRef]
86. Csillik, O.; Cherbini, J.; Johnson, R.; Lyons, A.; Kelly, M. Identification of Citrus Trees from Unmanned Aerial Vehicle Imagery Using Convolutional Neural Networks. *Drones* **2018**, *2*, 39. [CrossRef]
87. Ferreira, M.P.; de Almeida, D.R.A.; de Almeida Papa, D.; Minervino, J.B.S.; Veras, H.F.P.; Formighieri, A.; Santos, C.A.N.; Ferreira, M.A.D.; Figueiredo, E.O.; Ferreira, E.J.L. Individual tree detection and species classification of Amazonian palms using UAV images and deep learning. *For. Ecol. Manag.* **2020**, *475*, 118397. [CrossRef]
88. Liu, J.; Xiang, J.; Jin, Y.; Liu, R.; Yan, J.; Wang, L. Boost precision agriculture with unmanned aerial vehicle remote sensing and edge intelligence: A survey. *Remote Sens.* **2021**, *13*, 4387. [CrossRef]
89. Lin, C.; Jin, Z.; Mulla, D.; Ghosh, R.; Guan, K.; Kumar, V.; Cai, Y. Toward large-scale mapping of tree crops with high-resolution satellite imagery and deep learning algorithms: A case study of olive orchards in Morocco. *Remote Sens.* **2021**, *13*, 1740. [CrossRef]
90. Sibbett, G.S. Pruning mature bearing olive trees. In *Olive Production Manual*; Sibbett, G.S., Ferguson, L., Eds.; University of California, Agriculture and Natural Resources: Oakalnd, CA, USA, 2005; pp. 55–59.
91. García-Ortiz, A.; Humanes, J.; Pastor, M.; Morales, J.; Fernández, A. Poda. In *El Cultivo del Olivo*; Barranco, D., Fernández-Escobar, R., Rallo, L., Eds.; Coedición Junta de Andalucía (Consejería de Agricultura Y Pesca) & Mundi- Prensa: Madrid, Spain, 2008; pp. 389–433.
92. Rallo, L.; Díez, C.M.; Morales-sillero, A.; Miho, H. Quality of olives: A focus on agricultural preharvest factors. *Sci. Hortic.* **2018**, *233*, 491–509. [CrossRef]
93. Castillo-Ruiz, F.J.; Sola-Guirado, R.R.; Castro-Garcia, S.; Gonzalez-Sanchez, E.J.; Colmenero-Martinez, J.T.; Blanco-Roldán, G.L. Pruning systems to adapt traditional olive orchards to new integral harvesters. *Sci. Hortic.* **2017**, *220*, 122–129. [CrossRef]
94. Tous, J.; Romero, A.; Hermoso, J.F.; Msallem, M.; Larbi, A. Olive orchard design and mechanization: Present and future. *Acta Hortic.* **2014**, *1057*, 231–246. [CrossRef]
95. Palese, A.M.; Pergola, M.; Favia, M.; Xiloyannis, C.; Celano, G. A sustainable model for the management of olive orchards located in semi-arid marginal areas: Some remarks and indications for policy makers. *Environ. Sci. Policy* **2013**, *27*, 81–90. [CrossRef]
96. Rallo, L.; Barranco, D.; Castro-García, S.; Connor, D.J.; del Campo, M.G.; Rallo, P. High-density olive plantations. *Hortic. Rev. (Am. Soc. Hortic. Sci).* **2013**, *41*, 303–383. [CrossRef]
97. Tombesi, A.; Farinelli, D.; Ruffolo, M.; Sforna, A. First results of olive mechanical pruning. *Acta Hortic.* **2012**, *949*, 409–414. [CrossRef]
98. Marino, G.; Macaluso, L.; Grilo, F.; Marra, F.P.; Caruso, T. Toward the valorization of olive (*Olea europaea* var. *europaea* L.) biodiversity: Horticultural performance of seven Sicilian cultivars in a hedgerow planting system. *Sci. Hortic.* **2019**, *256*, 108583. [CrossRef]
99. International Olive Council. *Production Techniques in Olive Growing*, 1st ed.; International Olive Council: Madrid, Spain, 2007.
100. De Gennaro, B.; Notarnicola, B.; Roselli, L.; Tassielli, G. Innovative olive-growing models: An environmental and economic assessment. *J. Clean. Prod.* **2012**, *28*, 70–80. [CrossRef]
101. Sola-Guirado, R.R.; Aragon-Rodriguez, F.; Castro-Garcia, S.; Gil-Ribes, J. The vibration behaviour of hedgerow olive trees in response to mechanical harvesting with straddle harvester. *Biosyst. Eng.* **2019**, *184*, 81–89. [CrossRef]
102. Ferguson, L.; Glozer, K.; Crisosto, C.; Rosa, U.A.; Castro-Garcia, S.; Fichtner, E.J.; Guinard, J.X.; Lee, S.M.; Krueger, W.H.; Miles, J.A.; et al. Improving canopy contact olive harvester efficiency with mechanical pruning. *Acta Hortic.* **2012**, *965*, 83–88. [CrossRef]
103. Dias, A.B.; Peça, J.O.; Pinheiro, A. Long-term evaluation of the influence of mechanical pruning on olive growing. *Agron. J.* **2012**, *104*, 22–25. [CrossRef]

104. Connor, D.J.; Gómez-del-Campo, M.; Rousseaux, M.C.; Searles, P.S. Structure, management and productivity of hedgerow olive orchards: A review. *Sci. Hortic.* **2014**, *169*, 71–93. [CrossRef]
105. Estornell, J.; Velázquez-Martí, B.; López-Cortés, I.; Salazar, D.; Fernández-Sarría, A. Estimation of wood volume and height of olive tree plantations using airborne discrete-return LiDAR data. *GIScience Remote Sens.* **2014**, *51*, 17–29. [CrossRef]
106. Hadas, E.; Borkowski, A.; Estornell, J.; Tymkow, P. Automatic estimation of olive tree dendrometric parameters based on airborne laser scanning data using alpha-shape and principal component analysis. *GIScience Remote Sens.* **2017**, *54*, 898–917. [CrossRef]
107. Therios, I. *Olives: Crop Production Science in Horticulture 18*; CABI International: Wallingford, UK, 2009.
108. Jiménez-Brenes, F.M.; López-Granados, F.; de Castro, A.I.; Torres-Sánchez, J.; Serrano, N.; Peña, J.M. Quantifying pruning impacts on olive tree architecture and annual canopy growth by using UAV-based 3D modelling. *Plant Methods* **2017**, *13*, 55. [CrossRef] [PubMed]
109. Hadaś, E.; Estornell, J. Accuracy of tree geometric parameters depending on the liDAR data density. *Eur. J. Remote Sens.* **2016**, *49*, 73–92. [CrossRef]
110. Thenkabail, P.S. *Land Resources Monitoring, Modeling, and Mapping with Remote Sensing—Remote Sensing Handbook*, 1st ed.; CRC Press: Boca Raton, FL, USA, 2015; Volume II.
111. Edelsbrunner, H.; Kirkpatrick, D.G.; Seidel, R. On the shape of a set of points in the plane. *IEEE Trans. Inf. Theory* **1983**, *29*, 551–559. [CrossRef]
112. Repullo, M.A.; Carbonell, R.; Hidalgo, J.; Rodríguez-Lizana, A.; Ordóñez, R. Using olive pruning residues to cover soil and improve fertility. *Soil Tillage Res.* **2012**, *124*, 36–46. [CrossRef]
113. Estornell, J.; Ruiz, L.A.; Velázquez-Martí, B.; López-Cortés, I.; Salazar, D.; Fernández-Sarría, A. Estimation of pruning biomass of olive trees using airborne discrete-return LiDAR data. *Biomass and Bioenergy* **2015**, *81*, 315–321. [CrossRef]
114. Connor, D.J. Towards optimal designs for hedgerow olive orchards. *Aust. J. Agric. Res.* **2006**, *57*, 1067–1072. [CrossRef]
115. Caruso, G.; Palai, G.; Marra, F.P.; Caruso, T. High-resolution UAV imagery for field olive (*Olea europaea* L.) phenotyping. *Horticulturae* **2021**, *7*, 258. [CrossRef]
116. Tous, J.; Romero, A.; Plana, J.; Baiges, F. Planting density trial with "Arbequina" olive cultivar in Catalonia (Spain). *Acta Hortic.* **1999**, *474*, 177–180. [CrossRef]
117. Guerfel, M.; Ouni, Y.; Boujnah, D.; Zarrouk, M. Effects of the planting density on water relations and production of "Chemlali" olive trees (*Olea europaea* L.). *Trees-Struct. Funct.* **2010**, *24*, 1137–1142. [CrossRef]
118. Msallem, M.A.; Larbi, M.; Ayadi, A.; Dhiab, B.; Caballero, J. Influence of planting densities on the behavior of 'Arbequina' olive variety. In Proceedings of the The Sixth International Symposium on Olive Growing, Évora, Portugal, 9–13 September 2008; Book of Abstracts. p. 181.
119. Villalobos, F.J.; Testi, L.; Hidalgo, J.; Pastor, M.; Orgaz, F. Modelling potential growth and yield of olive (Olea europaea L.) canopies. *Eur. J. Agron.* **2006**, *24*, 296–303. [CrossRef]
120. Maselli, F.; Chiesi, M.; Brilli, L.; Moriondo, M. Simulation of olive fruit yield in Tuscany through the integration of remote sensing and ground data. *Ecol. Modell.* **2012**, *244*, 1–12. [CrossRef]
121. Peng, Y.; Zhu, T.; Li, Y.; Dai, C.; Fang, S.; Gong, Y.; Wu, X.; Zhu, R.; Liu, K. Remote prediction of yield based on LAI estimation in oilseed rape under different planting methods and nitrogen fertilizer applications. *Agric. For. Meteorol.* **2019**, *271*, 116–125. [CrossRef]
122. Sishodia, R.P.; Ray, R.L.; Singh, S.K. Applications of remote sensing in precision agriculture: A review. *Remote Sens.* **2020**, *12*, 3136. [CrossRef]
123. Stateras, D.; Kalivas, D. Assessment of olive tree canopy characteristics and yield forecast model using high resolution UAV imagery. *Agriculture* **2020**, *10*, 385. [CrossRef]
124. Peng, D.; Wu, C.; Li, C.; Zhang, X.; Liu, Z.; Ye, H.; Luo, S.; Liu, X.; Hu, Y.; Fang, B. Spring green-up phenology products derived from MODIS NDVI and EVI: Intercomparison, interpretation and validation using National Phenology Network and AmeriFlux observations. *Ecol. Indic.* **2017**, *77*, 323–336. [CrossRef]
125. Wu, C.; Peng, D.; Soudani, K.; Siebicke, L.; Gough, C.M.; Arain, M.A.; Bohrer, G.; Lafleur, P.M.; Peichl, M.; Gonsamo, A.; et al. Land surface phenology derived from normalized difference vegetation index (NDVI) at global FLUXNET sites. *Agric. For. Meteorol.* **2017**, *233*, 171–182. [CrossRef]
126. Lee, M.A.; Monteiro, A.; Barclay, A.; Marcar, J.; Miteva-Neagu, M.; Parker, J. A framework for predicting soft-fruit yields and phenology using embedded, networked microsensors, coupled weather models and machine-learning techniques. *Comput. Electron. Agric.* **2020**, *168*, 105103. [CrossRef]
127. Almeida, J.; dos Santos, J.A.; Alberton, B.; da S. Torres, R.; Morellato, L.P.C. Applying machine learning based on multiscale classifiers to detect remote phenology patterns in Cerrado savanna trees. *Ecol. Inform.* **2014**, *23*, 49–61. [CrossRef]
128. Azpiroz, I.; Oses, N.; Quartulli, M.; Olaizola, I.G.; Guidotti, D.; Marchi, S. Comparison of climate reanalysis and remote-sensing data for predicting olive phenology through machine-learning methods. *Remote Sens.* **2021**, *13*, 1224. [CrossRef]
129. Veroustraete, F.; Sabbe, H.; Eerens, H. Estimation of carbon mass fluxes over Europe using the C-Fix model and Euroflux data. *Remote Sens. Environ.* **2002**, *83*, 376–399. [CrossRef]
130. Running, S.W.; Hunt, E.R. *Generalization of a Forest Ecosystem Process Model for Other Biomes, BIOME-BGC, and an Application for Global-Scale Models*; Academic Press Inc.: San Diego, USA, 1993.

131. Brilli, L.; Chiesi, M.; Maselli, F.; Moriondo, M.; Gioli, B.; Toscano, P.; Zaldei, A.; Bindi, M. Simulation of olive grove gross primary production by the combination of ground and multi-sensor satellite data. *Int. J. Appl. Earth Obs. Geoinf.* **2013**, *23*, 29–36. [CrossRef]
132. Kölle, W.; Martínez Salgueiro, A.; Buchholz, M.; Musshoff, O. Can satellite-based weather index insurance improve the hedging of yield risk of perennial non-irrigated olive trees in Spain? *Aust. J. Agric. Resour. Econ.* **2021**, *65*, 66–93. [CrossRef]
133. Sola-Guirado, R.R.; Castillo-Ruiz, F.J.; Jiménez-Jiménez, F.; Blanco-Roldan, G.L.; Castro-Garcia, S.; Gil-Ribes, J.A. Olive actual "on year" yield forecast tool based on the tree canopy geometry using UAS imagery. *Sensors* **2017**, *17*, 1743. [CrossRef]
134. Ortenzi, L.; Violino, S.; Pallottino, F.; Figorilli, S.; Vasta, S.; Tocci, F.; Antonucci, F.; Imperi, G.; Costa, C. Early estimation of olive production from light drone orthophoto, through canopy radius. *Drones* **2021**, *5*, 118. [CrossRef]
135. Sankaran, S.; Khot, L.R.; Espinoza, C.Z.; Jarolmasjed, S.; Sathuvalli, V.R.; Vandemark, G.J.; Miklas, P.N.; Carter, A.H.; Pumphrey, M.O.; Knowles, N.R.; et al. Low-altitude, high-resolution aerial imaging systems for row and field crop phenotyping: A review. *Eur. J. Agron.* **2015**, *70*, 112–123. [CrossRef]
136. Rallo, L.; Barranco, D.; Díez, C.M.; Rallo, P.; Suárez, M.P.; Trapero, C.; Fernando, P.-A. Strategies for Olive (Olea europaea L.) Breeding: Cultivated Genetic Resources and Crossbreeding. In *Advances in Plant Breeding Strategies: Fruits*; Springer International Publishing: New York City, NY, USA, 2018; ISBN 9783319919447.
137. Gómez-Gálvez, F.J.; Pérez-Mohedano, D.; de la Rosa-Navarro, R.; Belaj, A. High-throughput analysis of the canopy traits in the worldwide olive germplasm bank of Córdoba using very high-resolution imagery acquired from unmanned aerial vehicle (UAV). *Sci. Hortic.* **2021**, *278*, 109851. [CrossRef]
138. Stillitano, T.; De Luca, A.I.; Falcone, G.; Spada, E.; Gulisano, G.; Strano, A. Economic profitability assessment of mediterranean olive growing systems. *Bulg. J. Agric. Sci.* **2016**, *22*, 517–526.
139. De La Rosa, R.; Kiran, A.I.; Barranco, D.; León, L. Seedling height as a pre-selection criterion for short juvenile period in olive seedlings. *Aust. J. Agric. Res.* **2006**, *57*, 477–481. [CrossRef]
140. Rallo, P.; de Castro, A.I.; López-Granados, F.; Morales-Sillero, A.; Torres-Sánchez, J.; Jiménez, M.R.; Jiménez-Brenes, F.M.; Casanova, L.; Suárez, M.P. Exploring UAV-imagery to support genotype selection in olive breeding programs. *Sci. Hortic.* **2020**, *273*, 109615. [CrossRef]
141. Hammami, S.B.M.; De la Rosa, R.; Sghaier-Hammami, B.; León, L.; Rapoport, H.F. Reliable and relevant qualitative descriptors for evaluating complex architectural traits in olive progenies. *Sci. Hortic.* **2012**, *143*, 157–166. [CrossRef]
142. Caruso, G.; Gucci, R.; Sifola, M.I.; Selvaggini, R.; Urbani, S.; Esposto, S.; Taticchi, A.; Servili, M. Irrigation and Fruit Canopy Position Modify Oil Quality of Olive Trees (cv. Frantoio). *J. Sci. Food Agric.* **2017**, *97*, 3530–3539. [CrossRef]
143. Torres-Sánchez, J.; de la Rosa, R.; León, L.; Jiménez-Brenes, F.M.; Kharrat, A.; López-Granados, F. Quantification of dwarfing effect of different rootstocks in 'Picual' olive cultivar using UAV-photogrammetry. *Precis. Agric.* **2021**, *23*, 178–193. [CrossRef]
144. Yang, G.; Liu, J.; Zhao, C.; Li, Z.; Huang, Y.; Yu, H.; Xu, B.; Yang, X.; Zhu, D.; Zhang, X.; et al. Unmanned aerial vehicle remote sensing for field-based crop phenotyping: Current status and perspectives. *Front. Plant Sci.* **2017**, *8*, 1111. [CrossRef]
145. Díaz-Varela, R.A.; de la Rosa, R.; León, L.; Zarco-Tejada, P.J. High-resolution airborne UAV imagery to assess olive tree crown parameters using 3D photo reconstruction: Application in breeding trials. *Remote Sens.* **2015**, *7*, 4213–4232. [CrossRef]
146. Miranda-Fuentes, A.; Llorens, J.; Gamarra-Diezma, J.L.; Gil-Ribes, J.A.; Gil, E. Towards an optimized method of olive tree crown volume measurement. *Sensors* **2015**, *15*, 3672–3687. [CrossRef]
147. Tattaris, M.; Reynolds, M.P.; Chapman, S.C. A direct comparison of remote sensing approaches for high-throughput phenotyping in plant breeding. *Front. Plant Sci.* **2016**, *7*, 1131. [CrossRef]
148. De Castro, A.I.; Rallo, P.; Suárez, M.P.; Torres-Sánchez, J.; Casanova, L.; Jiménez-Brenes, F.M.; Morales-Sillero, A.; Jiménez, M.R.; López-Granados, F. High-Throughput System for the Early Quantification of Major Architectural Traits in Olive Breeding Trials Using UAV Images and OBIA Techniques. *Front. Plant Sci.* **2019**, *10*, 1472. [CrossRef]
149. Avola, G.; Di Gennaro, S.F.; Cantini, C.; Riggi, E.; Muratore, F.; Tornambè, C.; Matese, A. Remotely sensed vegetation indices to discriminate field-grown olive cultivars. *Remote Sens.* **2019**, *11*, 1242. [CrossRef]
150. Jordan, C.F. Derivation of Leaf-Area Index from Quality of Light on the Forest Floor. *Ecology* **1969**, *50*, 663–666. [CrossRef]
151. Gitelson, A.A.; Kaufman, Y.J.; Merzlyak, M.N. Use of a green channel in remote sensing of global vegetation from EOS- MODIS. *Remote Sens. Environ.* **1996**, *58*, 289–298. [CrossRef]
152. Wang, F.; Huang, J.; Tang, Y.; Wang, X. New Vegetation Index and Its Application in Estimating Leaf Area Index of Rice. *Rice Sci.* **2007**, *14*, 195–203. [CrossRef]
153. Sripada, R.P.; Heiniger, R.W.; White, J.G.; Weisz, R. Aerial Color Infrared Photography for Determining Late-Season Nitrogen Requirements in Corn. *Agron. J.* **2005**, *97*, 1443–1451. [CrossRef]
154. Tucker, C.J. Red and photographic infrared linear combinations for monitoring vegetation. *Remote Sens. Environ.* **1979**, *8*, 127–150. [CrossRef]
155. Richardson, A.J.; Wiegand, C.L. Distinguishing vegetation from soil background information. *Photogramm. Eng. Remote Sens.* **1977**, *43*, 1541–1552.
156. Fernandez-Escobar, R.; de la Rosa, R.; Leon, L.; Gomez, J.A.; Testi, L.; Orgaz, F.; Gil- Ribes, J.A.; Quesada-moraga, E.; Trapero-Casas, A. Evolution and sustainability of the olive production systems. *Options Mediterr.* **2013**, *106*, 11–42.
157. León, L.; de la Rosa, R.; Barranco, D.; Rallo, L. Breeding for Early Bearing in Olive. *HortScience* **2007**, *42*, 499–502. [CrossRef]
158. Torres-Sánchez, J.; López-Granados, F.; Serrano, N.; Arquero, O.; Peña, J.M. High-throughput 3-D monitoring of agricultural-tree plantations with Unmanned Aerial Vehicle (UAV) technology. *PLoS ONE* **2015**, *10*, e0130479. [CrossRef]

159. Jurado, J.M.; Ortega, L.; Cubillas, J.J.; Feito, F.R. Multispectral mapping on 3D models and multi-temporal monitoring for individual characterization of olive trees. *Remote Sens.* **2020**, *12*, 1106. [CrossRef]
160. Westoby, M.J.; Brasington, J.; Glasser, N.F.; Hambrey, M.J.; Reynolds, J.M. "Structure-from-Motion" photogrammetry: A low-cost, effective tool for geoscience applications. *Geomorphology* **2012**, *179*, 300–314. [CrossRef]
161. Zarco-Tejada, P.J.; Diaz-Varela, R.; Angileri, V.; Loudjani, P. Tree height quantification using very high resolution imagery acquired from an unmanned aerial vehicle (UAV) and automatic 3D photo-reconstruction methods. *Eur. J. Agron.* **2014**, *55*, 89–99. [CrossRef]
162. Torres-Sánchez, J.; López-Granados, F.; Borra-Serrano, I.; Peña, J.M. Assessing UAV-collected image overlap influence on computation time and digital surface model accuracy in olive orchards. *Precis. Agric.* **2018**, *19*, 115–133. [CrossRef]
163. Woebbecke, D.; Meyer, G.; Von Bargen, K.; Mortensen, D. Shape features for identifying young weeds using image analysis. *Trans. Am. Soc. Agric. Eng.* **1995**, *38*, 270–281. [CrossRef]
164. Caruso, G.; Zarco-Tejada, P.J.; González-Dugo, V.; Moriondo, M.; Tozzini, L.; Palai, G.; Rallo, G.; Hornero, A.; Primicerio, J.; Gucci, R. High-resolution imagery acquired from an unmanned platform to estimate biophysical and geometrical parameters of olive trees under different irrigation regimes. *PLoS ONE* **2019**, *14*, e0210804. [CrossRef]
165. Gamon, J.A.; Peñuelas, J.; Field, C.B. A narrow-waveband spectral index that tracks diurnal changes in photosynthetic efficiency. *Remote Sens. Environ.* **1992**, *41*, 35–44. [CrossRef]
166. Haboudane, D.; Miller, J.R.; Tremblay, N.; Zarco-Tejada, P.J.; Dextraze, L. Integrated narrow-band vegetation indices for prediction of crop chlorophyll content for application to precision agriculture. *Remote Sens. Environ.* **2002**, *81*, 416–426. [CrossRef]
167. Rondeaux, G.; Steven, M.; Baret, F. Optimization of soil-adjusted vegetation indices. *Remote Sens. Environ.* **1996**, *55*, 95–107. [CrossRef]
168. Zarco-Tejada, P.J.; Miller, J.R.; Morales, A.; Berjón, A.; Agüera, J. Hyperspectral indices and model simulation for chlorophyll estimation in open-canopy tree crops. *Remote Sens. Environ.* **2004**, *90*, 463–476. [CrossRef]
169. Anifantis, A.S.; Camposeo, S.; Vivaldi, G.A.; Santoro, F.; Pascuzzi, S. Comparison of UAV photogrammetry and 3D modeling techniques with other currently used methods for estimation of the tree row volume of a super-high-density olive orchard. *Agriculture* **2019**, *9*, 233. [CrossRef]
170. Codis, S.; Carra, M.; Delpuech, X.; Montegano, P.; Nicot, H.; Ruelle, B.; Ribeyrolles, X.; Savajols, B.; Vergès, A.; Naud, O. Dataset of spray deposit distribution in vine canopy for two contrasted performance sprayers during a vegetative cycle associated with crop indicators (LWA and TRV). *Data Br.* **2018**, *18*, 415–421. [CrossRef]
171. Gitelson, A.A.; Kaufman, Y.J.; Stark, R.; Rundquist, D. Novel algorithms for remote estimation of vegetation fraction. *Remote Sens. Environ.* **2002**, *80*, 76–87. [CrossRef]
172. Mariscal, M.J.; Orgaz, F.; Villalobos, F.J. Modelling and measurement of radiation interception by olive canopies. *Agric. For. Meteorol.* **2000**, *100*, 183–197. [CrossRef]
173. Guillén-Climent, M.L.; Zarco-Tejada, P.J.; Villalobos, F.J. Estimating radiation interception in an olive orchard using physical models and multispectral airborne imagery. *Isr. J. Plant Sci.* **2012**, *60*, 107–121. [CrossRef]
174. North, P.R.J. Three-dimensional forest light interaction model using a monte carlo method. *IEEE Trans. Geosci. Remote Sens.* **1996**, *34*, 946–956. [CrossRef]
175. Noguera, M.; Aquino, A.; Ponce, J.M.; Cordeiro, A.; Silvestre, J.; Calderón, R.; da Encarnação Marcelo, M.; Jordão, P.; Andújar, J.M. Nutritional status assessment of olive crops by means of the analysis and modelling of multispectral images taken with UAVs. *Biosyst. Eng.* **2021**, *211*, 1–18. [CrossRef]
176. Gómez, J.A.; Zarco-Tejada, P.J.; García-Morillo, J.; Gama, J.; Soriano, M.A. Determining biophysical parameters for olive trees using CASI-airborne and QuickBird-satellite imagery. *Agron. J.* **2011**, *103*, 644–654. [CrossRef]
177. Molina, I.; Morillo, C.; García-Meléndez, E.; Guadalupe, R.; Roman, M.I. Characterizing olive grove canopies by Means of Ground-Based Hemispherical Photography and spaceborne RADAR data. *Sensors* **2011**, *11*, 7476–7501. [CrossRef]
178. Abdelmoula, H.; Kallel, A.; Roujean, J.L.; Chaabouni, S.; Gargouri, K.; Ghrab, M.; Gastellu-Etchegorry, J.P.; Lauret, N. Olive biophysical property estimation based on Sentinel-2 image inversion. In Proceedings of the 2018 IEEE International Geoscience and Remote Sensing Symposium, Valencia, Spain, 22–27 July 2018; pp. 2869–2872. [CrossRef]
179. Selby, S.M. *CRC Standard Mathematical Tables*; CRC Press: Cleveland, OH, USA, 1973.
180. Robert, C.P.; Casella, G. Monte Carlo Statistical Methods. *Technometrics* **2000**, *42*, 430. [CrossRef]
181. Moreira, B.M.; Goyanes, G.; Pina, P.; Vassilev, O.; Heleno, S. Assessment of the influence of survey design and processing choices on the accuracy of tree diameter at breast height (Dbh) measurements using uav-based photogrammetry. *Drones* **2021**, *5*, 43. [CrossRef]
182. Ehsani, R.; Maja, J.M. The rise of small UAVs in precision agriculture. *Resour. Eng. Technol. Sustain. World* **2013**, *20*, 18–19.
183. Calderón, R.; Navas-Cortés, J.A.; Lucena, C.; Zarco-Tejada, P.J. High-resolution airborne hyperspectral and thermal imagery for early detection of Verticillium wilt of olive using fluorescence, temperature and narrow-band spectral indices. *Remote Sens. Environ.* **2013**, *139*, 231–245. [CrossRef]
184. Reynolds, G.J.; Windels, C.E.; MacRae, I.V.; Laguette, S. Remote sensing for assessing Rhizoctonia crown and root rot severity in sugar beet. In Proceedings of the 36th Biennial Meeting, ASSBT, Albuquerque, NM, USA, 2–5 March 2011.
185. Calamita, F.; Imran, H.A.; Vescovo, L.; Mekhalfi, M.L.; La Porta, N. Early Identification of Root Rot Disease by Using Hyperspectral Reflectance: The Case of Pathosystem Grapevine/Armillaria. *Remote Sens.* **2021**, *13*, 2436. [CrossRef]

186. Wells, J.M.; Raju, B.C.; Hung, H.-Y.; Weisburg, W.G.; Mandelco-Paul, L.; Brenner, D.J. Xylella fastidiosa gen. nov., sp. nov: Gram-Negative, Xylem-Limited, Fastidious Plant Bacteria Related to *Xanthomonas* spp. *Int. J. Syst. Bacteriol.* **1987**, *37*, 136–143. [CrossRef]
187. Schreiber, L.; Green, R.J.J. Effect of root exudates on germination of conidia and microsclerotia of Verticillium alboatrum inhibited by the soil fungistatic principle. *Phytopathology* **1963**, *53*, 260–264.
188. Ayres, P. *Water Relations of Diseased Plants*; Academic Press: London, UK, 1978; Volume 5.
189. DeVay, J. Selection, characterization, pathogenicity and virulence of pectinase- deficient mutants of Verticillium albo-atrum. In *Vascular Wilt Diseases of Plants*; Beckman, C., Tjamos, E., Eds.; Springer: Berlin/Heidelberg, Germany, 1989; pp. 197–217.
190. Van Alfen, N. Reassessment of plant wilt toxins. *Annu. Rev. Phytopathol.* **1989**, *27*, 533–550. [CrossRef]
191. Navas-Cortés, J.A.; Landa, B.B.; Mercado-Blanco, J.; Trapero-Casas, J.L.; Rodríguez-Jurado, D.; Jiménez-Díaz, R.M. Spatiotemporal analysis of spread of infections by Verticillium dahliae pathotypes within a high tree density olive orchard in Southern Spain. *Phytopathology* **2008**, *98*, 167–180. [CrossRef]
192. Hiemstra, J.; Harris, D. *A Compendium of Verticillium Wilts in Tree Species*; CPRO: Hong Kong, China, 1998; ISBN 9073771250.
193. Steiner, U.; Buerling, K.; Oerke, E.-C. Sensor use in plant protection. *Gesunde Pflanz.* **2008**, *60*, 131–141. [CrossRef]
194. Montes Osuna, N.M.; Mercado-Blanco, J. Verticillium Wilt of Olive and Its Control: What Did We Learn during the Last Decade. *Plants* **2020**, *9*, 735. [CrossRef] [PubMed]
195. Hillnhutter, C.; Schweizer, A.; Volker, K.; Sikora, R.A. Remote Sensing for the Detection of Soil-Borne Plant Parasitic Nematodes and Fungal Pathogens. In *Precision Crop Protection—The Challenge and Use of Heterogeneity*; Springer: Berlin/Heidelberg, Germany, 2010; pp. 151–165. ISBN 9789048192779.
196. Messina, G.; Modica, G. Applications of UAV thermal imagery in precision agriculture: State of the art and future research outlook. *Remote Sens.* **2020**, *12*, 1491. [CrossRef]
197. Idso, S.B.; Jackson, R.D.; Pinter, P.J.; Reginato, R.J.; Hatfield, J.L. Normalizing the stress-degree-day parameter for environmental variability. *Agric. Meteorol.* **1981**, *24*, 45–55. [CrossRef]
198. Calderón, R.; Navas-Cortés, J.A.; Zarco-Tejada, P.J. Early detection and quantification of verticillium wilt in olive using hyperspectral and thermal imagery over large areas. *Remote Sens.* **2015**, *7*, 5584–5610. [CrossRef]
199. Blekos, K.; Tsakas, A.; Xouris, C.; Evdokidis, I.; Alexandropoulos, D.; Alexakos, C.; Katakis, S.; Makedonas, A.; Theoharatos, C.; Lalos, A. Analysis, modeling and multi-spectral sensing for the predictive management of verticillium wilt in olive groves. *J. Sens. Actuator Netw.* **2021**, *10*, 15. [CrossRef]
200. Iatrou, G.; Mourelatos, S.; Zartaloudis, Z.; Iatrou, M.; Gewehr, S.; Kalaitzopoulou, S. Remote sensing for the management of Verticillium wilt of olive. *Fresenius Environ. Bull.* **2016**, *25*, 3622–3628.
201. Gitelson, A. Nondestructive Estimation of Foliar Pigment (Chlorophylls, Carotenoids, and Anthocyanins) Contents. In *Hyperspectral Remote Sensing of Vegetation*; CRC Press: Boca Raton, FL, USA, 2011; pp. 141–166. ISBN 1439845387.
202. Navrozidis, L.; Alexandridis, T.K.; Moshou, D.; Pantazi, X.E.; Alexandra Tamouridou, A.; Kozhukh, D.; Castef, F.; Lagopodi, A.; Zartaloudis, Z.; Mourelatos, S.; et al. Olive Trees Stress Detection Using Sentinel-2 Images. In Proceedings of the 2019 IEEE International Geoscience and Remote Sensing Symposium, Yokohama, Japan, 28 July–2 August 2019; pp. 7220–7223. [CrossRef]
203. Almeida, R.P.P.; Nunney, L. How do plant diseases caused by Xylella fastidiosa emerge? *Plant Dis.* **2015**, *99*, 1457–1467. [CrossRef]
204. Di Nisio, A.; Adamo, F.; Acciani, G.; Attivissimo, F. Fast detection of olive trees affected by xylella fastidiosa from uavs using multispectral imaging. *Sensors* **2020**, *20*, 4915. [CrossRef]
205. EFSA Panel on Plant Health (PLH). Treatment solutions to cure Xylella fastidiosa diseased plants. *EFSA J.* **2018**, *14*, e04456. [CrossRef]
206. Navarrete, F.; De La Fuente, L. Response of Xylella fastidiosa to zinc: Decreased culturability, increased exopolysaccharide production, and formation of resilient biofilms under flow conditions. *Appl. Environ. Microbiol.* **2014**, *80*, 1097–1107. [CrossRef]
207. Saponari, M.; Boscia, D.; Altamura, G.; Loconsole, G.; Zicca, S.; D'Attoma, G.; Morelli, M.; Palmisano, F.; Saponari, A.; Tavano, D.; et al. Isolation and pathogenicity of Xylella fastidiosa associated to the olive quick decline syndrome in southern Italy. *Sci. Rep.* **2017**, *7*, 17723. [CrossRef] [PubMed]
208. Girelli, C.R.; Del Coco, L.; Scortichini, M.; Petriccione, M.; Zampella, L.; Mastrobuoni, F.; Cesari, G.; Bertaccini, A.; D'Amico, G.; Contaldo, N.; et al. Xylella fastidiosa and olive quick decline syndrome (CoDiRO) in Salento (southern Italy): A chemometric 1H NMR-based preliminary study on Ogliarola salentina and Cellina di Nardò cultivars. *Chem. Biol. Technol. Agric.* **2017**, *4*, 25. [CrossRef]
209. Cornara, D.; Saponari, M.; Zeilinger, A.R.; de Stradis, A.; Boscia, D.; Loconsole, G.; Bosco, D.; Martelli, G.P.; Almeida, R.P.P.; Porcelli, F. Spittlebugs as vectors of Xylella fastidiosa in olive orchards in Italy. *J. Pest Sci.* **2017**, *90*, 521–530. [CrossRef]
210. Morelli, M.; García-Madero, J.M.; Jos, Á.; Saldarelli, P.; Dongiovanni, C.; Kovacova, M.; Saponari, M.; Arjona, A.B.; Hackl, E.; Webb, S.; et al. Xylella fastidiosa in olive: A review of control attempts and current management. *Microorganisms* **2021**, *9*, 1771. [CrossRef]
211. Giampetruzzi, A.; Morelli, M.; Saponari, M.; Loconsole, G.; Chiumenti, M.; Boscia, D.; Savino, V.N.; Martelli, G.P.; Saldarelli, P. Transcriptome profiling of two olive cultivars in response to infection by the CoDiRO strain of Xylella fastidiosa subsp. pauca. *BMC Genom.* **2016**, *17*, 475. [CrossRef] [PubMed]
212. Martelli, G.P. The current status of the quick decline syndrome of olive in southern Italy. *Phytoparasitica* **2016**, *44*, 1–10. [CrossRef]

213. Luvisi, A.; Aprile, A.; Sabella, E.; Vergine, M. Xylella fastidiosa subsp. pauca (CoDiRO strain) infection in four olive (*Olea europaea* L.) cultivars: Profile of phenolic compounds in leaves and progression of leaf scorch symptoms. *Phytopathol. Mediterr.* **2017**, *56*, 259–273. [CrossRef]
214. Raffini, F.; Bertorelle, G.; Biello, R.; D'Urso, G.; Russo, D.; Bosso, L. From nucleotides to satellite imagery: Approaches to identify and manage the invasive pathogen Xylella fastidiosa and its insect vectors in Europe. *Sustainability* **2020**, *12*, 4508. [CrossRef]
215. Bragard, C.; Dehnen-Schmutz, K.; Di Serio, F.; Gonthier, P.; Jacques, M.; Jaques Miret, J.A.; Justesen, A.F.; MacLeod, A.; Magnusson, C.S.; Milonas, P.; et al. Effectiveness of in planta control measures for Xylella fastidiosa. *EFSA J.* **2019**, *17*, e05666. [CrossRef]
216. Liccardo, A.; Fierro, A.; Garganese, F.; Picciotti, U.; Porcelli, F. A biological control model to manage the vector and the infection of Xylella fastidiosa on olive trees. *PLoS ONE* **2020**, *15*, e0232363. [CrossRef]
217. Poblete, T.; Camino, C.; Beck, P.S.A.; Hornero, A.; Kattenborn, T.; Saponari, M.; Boscia, D.; Navas-Cortes, J.A.; Zarco-Tejada, P.J. Detection of Xylella fastidiosa infection symptoms with airborne multispectral and thermal imagery: Assessing bandset reduction performance from hyperspectral analysis. *ISPRS J. Photogramm. Remote Sens.* **2020**, *162*, 27–40. [CrossRef]
218. Hornero, A.; Hernández-Clemente, R.; North, P.R.J.; Beck, P.S.A.; Boscia, D.; Navas-Cortes, J.A.; Zarco-Tejada, P.J. Monitoring the incidence of Xylella fastidiosa infection in olive orchards using ground-based evaluations, airborne imaging spectroscopy and Sentinel-2 time series through 3-D radiative transfer modelling. *Remote Sens. Environ.* **2020**, *236*, 111480. [CrossRef]
219. Zarco-Tejada, P.J.; Camino, C.; Beck, P.S.A.; Calderon, R.; Hornero, A.; Hernández-Clemente, R.; Kattenborn, T.; Montes-Borrego, M.; Susca, L.; Morelli, M.; et al. Previsual symptoms of Xylella fastidiosa infection revealed in spectral plant-trait alterations. *Nat. Plants* **2018**, *4*, 432–439. [CrossRef] [PubMed]
220. Felzenszwalb, P.F.; Huttenlocher, D.P. Efficient graph-based image segmentation. *Int. J. Comput. Vis.* **2004**, *59*, 167–181. [CrossRef]
221. Hornero, A.; Hernández-Clemente, R.; Beck, P.S.A.; Navas-Cortés, J.A.; Zarco-Tejada, P.J. Using sentinel-2 imagery to track changes produced by Xylella fastidiosa in olive trees. In Proceedings of the 2018 IEEE International Geoscience and Remote Sensing Symposium, Valencia, Spain, 22–27 July 2008; pp. 9060–9062. [CrossRef]
222. Bannari, A.; Morin, D.; Bonn, F.; Huete, A.R. A review of vegetation indices. *Remote Sens. Rev.* **1995**, *13*, 95–120. [CrossRef]
223. Castrignanò, A.; Belmonte, A.; Antelmi, I.; Quarto, R.; Quarto, F.; Shaddad, S.; Sion, V.; Muolo, M.R.; Ranieri, N.A.; Gadaleta, G.; et al. A geostatistical fusion approach using UAV data for probabilistic estimation of Xylella fastidiosa subsp. pauca infection in olive trees. *Sci. Total Environ.* **2021**, *752*, 141814. [CrossRef] [PubMed]
224. Doitsidis, L.; Fouskitakis, G.N.; Varikou, K.N.; Rigakis, I.I.; Chatzichristofis, S.A.; Papafilippaki, A.K.; Birouraki, A.E. Remote monitoring of the Bactrocera oleae (Gmelin) (Diptera: Tephritidae) population using an automated McPhail trap. *Comput. Electron. Agric.* **2017**, *137*, 69–78. [CrossRef]
225. Philimis, P.; Psimolophitis, E.; Hadjiyiannis, S.; Giusti, A.; Perelló, J.; Serrat, A.; Avila, P. A centralised remote data collection system using automated traps for managing and controlling the population of the Mediterranean (Ceratitis capitata) and olive (Dacus oleae) fruit flies. In Proceedings of the First International Conference on Remote Sensing and Geoinformation of the Environment, Paphos, Cyprus, 8–10 April 2013; Volume 8795, p. 87950. [CrossRef]
226. Tzanakakis, M. Seasonal development and dormancy of insects and mites feedinf on olive: A review. *Neth. J. Zool.* **2003**, *52*, 87–224. [CrossRef]
227. Gómez-Caravaca, A.M.; Cerretani, L.; Bendini, A.; Segura-Carretero, A.; Fernández-Gutiérrez, A.; Del Carlo, M.; Compagnone, D.; Cichelli, A. Effects of Fly Attack (*Bactrocera oleae*) on the Phenolic Profile and Selected Chemical Parameters of Olive Oil. *J. Agric. Food Chem.* **2008**, *56*, 4577–4583. [CrossRef]
228. Tamendjari, A.; Angerosa, F.; Mettouchi, S.; Bellal, M.M. The effect of fly attack (Bactrocera oleae) on the quality and phenolic content of Chemlal olive oil. *Grasas Aceites* **2009**, *60*, 507–513. [CrossRef]
229. Neuenschwander, P.; Michelakis, S. The infestation of Dacus oleae (Gmel.) (Diptera, Tephritidae) at harvest time and its influence on yield and quality of olive oil in Crete. *Z. Angew. Entomol.* **2009**, *86*, 420–433. [CrossRef]
230. Gucci, R.; Caruso, G.; Canale, A.; Loni, A.; Raspi, A.; Urbani, S.; Taticchi, A.; Esposto, S.; Servili, M. Qualitative changes of olive oils obtained from fruits damaged by Bactrocera oleae (Rossi). *HortScience* **2012**, *47*, 301–306. [CrossRef]
231. Dimou, I.; Koutsikopoulos, C.; Economopoulos, A.P.; Lykakis, J. Depth of pupation of the wild olive fruit fly, Bactrocera (Dacus) oleae (Gmel.) (Dipt., Tephritidae), as affected by soil abiotic factors. *J. Appl. Entomol.* **2003**, *127*, 12–17. [CrossRef]
232. Gonçalves, F.M.; Rodrigues, M.C.; Pereira, J.A.; Thistlewood, H.; Torres, L.M. Natural mortality of immature stages of Bactrocera oleae (Diptera: Tephritidae) in traditional olive groves from north-eastern Portugal. *Biocontrol Sci. Technol.* **2012**, *22*, 837–854. [CrossRef]
233. Economopoulos, A.P.; Haniotakis, G.E.; Michelakis, S.; Tsiropoulos, G.J.; Zervas, G.A.; Tsitsipis, J.A.; Manoukas, A.G.; Kiritsakis, A.; Kinigakis, P. Population studies on the olive fruit fly, Dacus oleae (Gmel.) (Dipt., Tephritidae) in Western Crete. *Zeitschrift für Angew. Entomol.* **1982**, *93*, 463–476. [CrossRef]
234. Avidov, Z. Further investigations on the ecology of the olive fly (Dacus oleae Gmel.) in Israel. *Ktavim* **1954**, *4*, 39–50.
235. Blum, M.; Lensky, I.M.; Rempoulakis, P.; Nestel, D. Modeling insect population fluctuations with satellite land surface temperature. *Ecol. Modell.* **2015**, *311*, 39–47. [CrossRef]
236. Blum, M.; Lensky, I.M.; Nestel, D. Estimation of olive grove canopy temperature from MODIS thermal imagery is more accurate than interpolation from meteorological stations. *Agric. For. Meteorol.* **2013**, *176*, 90–93. [CrossRef]
237. Caselli, A.; Petacchi, R. Climate Change and Major Pests of Mediterranean Olive Orchards: Are We Ready to Face the Global Heating? *Insects* **2021**, *12*, 802. [CrossRef]

238. Floreano, D.; Wood, R.J. Science, technology and the future of small autonomous drones. *Nature* **2015**, *521*, 460–466. [CrossRef]
239. Tsouros, D. A review on U. applications for precision agriculturemosthenis C.; Bibi, S.; Sarigiannidis, P.G. A review on UAV-based applications for precision agriculture. *Information* **2019**, *10*, 349. [CrossRef]
240. Barbedo, J.G.A. A review on the use of unmanned aerial vehicles and imaging sensors for monitoring and assessing plant stresses. *Drones* **2019**, *3*, 40. [CrossRef]
241. Sagan, V.; Maimaitiyiming, M.; Sidike, P.; Maimaitiyiming, M.; Erkbol, H.; Peterson, K.T.; Peterson, J.; Burken, J.; Fritschi, F. UAV/Satellite Multiscale Data Fusion for Crop Monitoring and Early Stress Detection. In Proceedings of the International Archives of the Photogrammetry, Remote Sensing and Spatial Information Sciences, Enschede, The Netherlands, 10–14 June 2019; Volume XLII-2/W13. [CrossRef]
242. Khan, N.; Ray, R.L.; Sargani, G.R.; Ihtisham, M.; Khayyam, M.; Ismail, S. Current progress and future prospects of agriculture technology: Gateway to sustainable agriculture. *Sustainability* **2021**, *13*, 4883. [CrossRef]
243. Radoglou-Grammatikis, P.; Sarigiannidis, P.; Lagkas, T.; Moscholios, I. A compilation of UAV applications for precision agriculture. *Comput. Netw.* **2020**, *172*, 107148. [CrossRef]
244. Kosior, K. Digital Transformation in the Agri-Food Sector—Opportunities and Challenges. *Ann. Polish Assoc. Agric. Agribus. Econ.* **2018**, *XX*, 98–104. [CrossRef]
245. Reichstein, M.; Camps-Valls, G.; Stevens, B.; Jung, M.; Denzler, J.; Carvalhais, N. Prabhat Deep learning and process understanding for data-driven Earth system science. *Nature* **2019**, *566*, 195–204. [CrossRef]
246. Vincini, M.; Frazzi, E.; D'Alessio, P. Comparison of narrow-band and broad-band vegetation indices for canopy chlorophyll density estimation in sugar beet. In Proceedings of the Precision Agriculture 2007—Papers Presented at the 6th European Conference on Precision Agriculture, ECPA 2007, Skiathos, Greece, 3–6 June 2007; pp. 189–196.
247. Liu, H.Q.; Huete, A. A feedback based modification of the NDVI to minimize canopy background and atmospheric noise. *IEEE Trans. Geosci. Remote Sens.* **1995**, *33*, 457–465. [CrossRef]
248. Jiang, Z.; Huete, A.; Didan, K.; Miura, T. Development of a two-band enhanced vegetation index without a blue band. *Remote Sens. Environ.* **2008**, *112*, 3833–3845. [CrossRef]
249. Wu, W. The Generalized Difference Vegetation Index (GDVI) for Dryland Characterization. *Remote Sens.* **2014**, *6*, 1211–1233. [CrossRef]
250. Gitelson, A.; Merzlyak, M.N. Spectral Reflectance Changes Associated with Autumn Senescence of Aesculus hippocastanum L. and Acer platanoides L. Leaves. Spectral Features and Relation to Chlorophyll Estimation. *J. Plant Physiol.* **1994**, *143*, 286–292. [CrossRef]
251. Chen, J.M. Evaluation of vegetation indices and a modified simple ratio for boreal applications. *Can. J. Remote Sens.* **1996**, *22*, 229–242. [CrossRef]
252. Berni, J.; Zarco-Tejada, P.J.; Sepulcre-Cantó, G.; Fereres, E.; Villalobos, F. Mapping canopy conductance and CWSI in olive orchards using high resolution thermal remote sensing imagery. *Remote Sens. Environ.* **2009**, *113*, 2380–2388. [CrossRef]
253. Poblete, T.; Navas-Cortes, J.A.; Camino, C.; Calderon, R.; Hornero, A.; Gonzalez-Dugo, V.; Landa, B.B.; Zarco-Tejada, P.J. Discriminating Xylella fastidiosa from Verticillium dahliae infections in olive trees using thermal- and hyperspectral-based plant traits. *ISPRS J. Photogramm. Remote Sens.* **2021**, *179*, 133–144. [CrossRef]
254. Roujean, J.L.; Breon, F.M. Estimating PAR absorbed by vegetation from bidirectional reflectance measurements. *Remote Sens. Environ.* **1995**, *51*, 375–384. [CrossRef]
255. Huete, A.R. A soil-adjusted vegetation index (SAVI). *Remote Sens. Environ.* **1988**, *25*, 295–309. [CrossRef]
256. Vogelmann, J.E.; Rock, B.N.; Moss, D.M. Red edge spectral measurements from sugar maple leaves. *Int. J. Remote Sens.* **1993**, *14*, 1563–1575. [CrossRef]
257. Yang, C. High resolution satellite imaging sensors for precision agriculture. *Front. Agric. Sci. Eng.* **2018**, *5*, 393–405. [CrossRef]
258. Urieta, D.; Menor, A.; Caño, S.; Barreal, J.; Del Mar Velasco, M.; Puentes, R. *International Olive Growing Worldwide Analysis and Summary*, 1st ed.; Fundación Caja Rural de Jaén: Jaén, Spain, 2018.
259. Romero-Gámez, M.; Castro-Rodríguez, J.; Suárez-Rey, E.M. Optimization of olive growing practices in Spain from a life cycle assessment perspective. *J. Clean. Prod.* **2017**, *149*, 25–37. [CrossRef]
260. Lombardo, L.; Farolfi, C.; Capri, E. Sustainability Certification, a New Path of Value Creation in the Olive Oil Sector: The ITALIAN Case Study. *Foods* **2021**, *10*, 501. [CrossRef]
261. Bartolini, G. Olive Germplasm (Olea europaea L.), Cultivars, Synonyms, Cultivation Area, Collections, Descriptors. Available online: http://www.oleadb.it/ (accessed on 11 April 2022).
262. Ozturk, M.; Altay, V.; Gönenç, T.M.; Unal, B.T.; Efe, R.; Akçiçek, E.; Bukhari, A. An Overview of Olive Cultivation in Turkey: Botanical Features, Eco-Physiology and Phytochemical Aspects. *Agronomy* **2021**, *11*, 295. [CrossRef]
263. Bernardi, B.; Falcone, G.; Stillitano, T.; Benalia, S.; Strano, A.; Bacenetti, J.; De Luca, A.I. Harvesting system sustainability in Mediterranean olive cultivation. *Sci. Total Environ.* **2018**, *625*, 1446–1458. [CrossRef] [PubMed]
264. Farinelli, D.; Onorati, L.; Ruffolo, M.; Tombesi, A. Mechanical pruning of adult olive trees and influence on yield and on efficiency on mechanical harvesting. *Acta Hortic.* **2011**, *924*, 203–209. [CrossRef]
265. Mairech, H.; López-Bernal, Á.; Moriondo, M.; Dibari, C.; Regni, L.; Proietti, P.; Villalobos, F.J.; Testi, L. Is new olive farming sustainable? A spatial comparison of productive and environmental performances between traditional and new olive orchards with the model OliveCan. *Agric. Syst.* **2020**, *181*, 102816. [CrossRef]

266. Navarro, C.; Hidalgo, J.; Gomez Del Campo, M. Sistemas de plantación. In *El Cultivo Del Olivo*; Mundi-Prensa Libros: Madrid, Spain, 2017; pp. 288–334.
267. Fraga, H.; Moriondo, M.; Leolini, L.; Santos, J.A. Mediterranean Olive Orchards under Climate Change: A Review of Future Impacts and Adaptation Strategies. *Agronomy* **2020**, *11*, 56. [CrossRef]
268. Servili, M.; Sordini, B.; Esposto, S.; Urbani, S.; Veneziani, G.; Di Maio, I.; Selvaggini, R.; Taticchi, A. Biological activities of phenolic compounds of extra virgin olive oil. *Antioxidants* **2014**, *3*, 1–13. [CrossRef] [PubMed]
269. Brito, C.; Dinis, L.; Moutinho-Pereira, J.; Correia, C.M. Drought Stress Effects and Olive Tree Acclimation under a Changing Climate. *Plants* **2019**, *8*, 232. [CrossRef]
270. Schwingshackl, L.; Christoph, M.; Hoffmann, G. Effects of Olive Oil on Markers of Inflammation and Endothelial Function—A Systematic Review and Meta-Analysis. *Nutrients* **2015**, *7*, 7651–7675. [CrossRef]